VOLUME 19, 1957/58, No. 7-8 pp. 209-244 Published 10th February 1958

Philips Technical Review

DEALING WITH TECHNICAL PROBLEMS
RELATING TO THE PRODUCTS, PROCESSES AND INVESTIGATIONS OF
THE PHILIPS INDUSTRIES

CRYSTAL-ORIENTED FERROXPLANA

by A. L. STUIJTS and H. P. J. WIJN.

621.318.13:538.213

The magnetically soft materials "ferroxplana", on which an article recently appeared in this Review, have a permeability which remains constant up to frequencies far above 100 Mc/s. It appears that the crystals of these materials can be aligned. As a result the permeability is appreciably increased, with only a slight drop in the limiting frequency. Moreover, this produces a material with an anisotropic permeability, for which there are special applications.

Introduction

A short time ago some new groups of ferromagnetic oxides were discovered in the Philips Laboratory, Eindhoven, which, like the earlier described material ferroxdure, possess a hexagonal crystalline structure. These materials were described in an article in this Review [1]), which we shall henceforth refer to as I. The composition of these compounds can be represented in a triangle diagram, the vertices of which are formed by three oxides. This triangle is shown in *fig. 1*. Me represents a divalent ion from the series Mn, Fe, Co, Ni, Cu, Zn, Mg, or a mixture of these ions. On the sides of the triangle are found the compound **B** ($BaFe_2O_4$), the group of compounds **S** ($MeFe_2O_4$, which includes ferroxcube) and the compound **M** ($BaFe_{12}O_{19}$, main constituent of ferroxdure). The new groups of compounds discussed in I are represented in the triangle by the points **W** ($BaMe_2Fe_{16}O_{27}$), **Y** ($Ba_2Me_2Fe_{12}O_{22}$) and **Z** ($Ba_3Me_2Fe_{24}O_{41}$). Later, the new groups of compounds **X** and **U** were discovered [2]). If, in the **Z** group, for example, the Co ion is chosen for Me, this compound can be briefly denoted by Co_2Z, indicating that the structural unit (this is not the unit cell, see I, ref. [7]) and p. 153) contains two Co ions.

As in the case of ferroxcube and ferroxdure, these materials are prepared by sintering at high tempera-

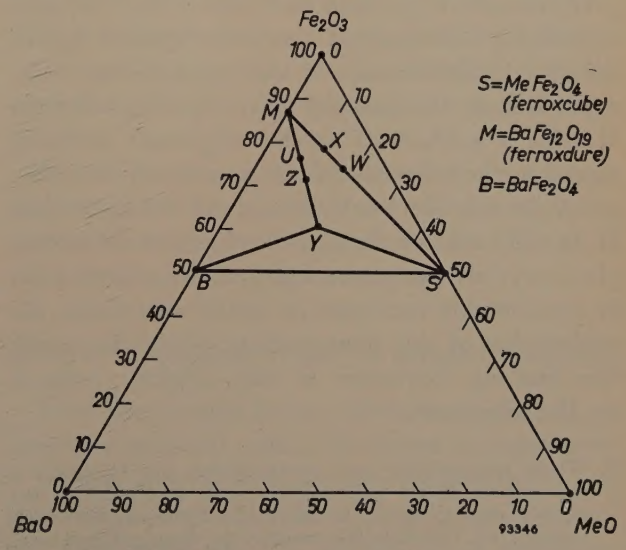

Fig. 1. The composition of the materials **W**, **Y**, **Z**, **X** and **U** can be represented by points in the triangle BaO-MeO-Fe_2O_3. **B**, **S** and **M** represent the known materials $BaFe_2O_4$, ferroxcube and ferroxdure, respectively.

[1]) G. H. Jonker, H. P. J. Wijn and P. B. Braun, Ferroxplana, hexagonal ferromagnetic iron-oxide compounds for very high frequencies, Philips tech. Rev. **18**, 145-154, 1956/57, (No. 6); referred to in this article as I.

[2]) See P. B. Braun, thesis, Amsterdam 1956, also Philips Res. Rep. **12**, 491-548, 1957 (No. 6); G. H. Jonker, Ferrimagnetic iron oxide compounds with hexagonal crystal structure, paper presented in June 1957 to 16e Congrès intern. Chimie pure et appl., Paris.

tures, which gives rise to a reaction between the constituent oxides and the atmosphere. The ceramic product so produced has a high resistivity (10^4-10^{10} ohm cm).

It has been found that in all compounds of the Y group, and also in those of the Z and W groups which contain more than a certain content of Co, the crystals exhibit a preferred plane for the magnetization; these compounds have been given the name ferroxplana. This preferred plane is perpendicular to the (hexagonal) *c*-axis, which we have called the "abhorred" direction. The magnetic anisotropy for rotations out of this plane is generally large, which is to say that the magnetization is very stiffly bound to this plane, and therefore the permeability in the direction perpendicular to the preferred plane is small. However, the magnetization can fairly easily be rotated in the preferred plane itself (relatively small anisotropy for rotations in the preferred plane) so that the permeability in directions parallel to this plane can be much higher [3]). In polycrystalline material, in which the preferred planes lie in arbitrary directions, there is then a certain average isotropic permeability. It was shown in I that, owing to the markedly differing anisotropies of the crystals, the product of the permeability and the frequency above which the losses show a sharp increase (limiting frequency) can attain a much higher value than with ferroxcube. For example, in the case of Co_2Z the permeability is found to be about 10 at a limiting frequency of about 400 Mc/s, while ferroxcube 4E with a permeability of 12 has a limiting frequency of about 90 Mc/s.

In this article we shall first discuss how the permeability of ferroxplana can be influenced by an anisotropic distribution of the orientations of the crystallites in the material (texture). We shall then describe a method of crystal alignment differing from a method described for ferroxdure in an earlier article in this Review [4]), henceforth referred to as II. It will be shown that by the alignment of ferroxplana crystals the permeability of the material can be considerably increased in certain directions; the explanation of this phenomenon will be discussed. The limiting frequency is only slightly reduced by the alignment.

[3]) Where permeability and susceptibility are referred to, the *relative initial* permeability and susceptibility are always meant (in μ_0 units in the rationalized Giorgi system), i.e. the value measured in the demagnetized state upon application of a very weak magnetic field.

[4]) A. L. Stuijts, G. W. Rathenau and G. H. Weber, Ferroxdure II and III, anisotropic permanent magnet materials, Philips tech. Rev. **16**, 141-147, 1954/55; referred to in this article as II.

Anisotropic ferroxplana materials

The most anisotropic material is the single crystal. The anisotropic magnetic properties of a ferroxplana single crystal are exemplified in *fig. 2*, where

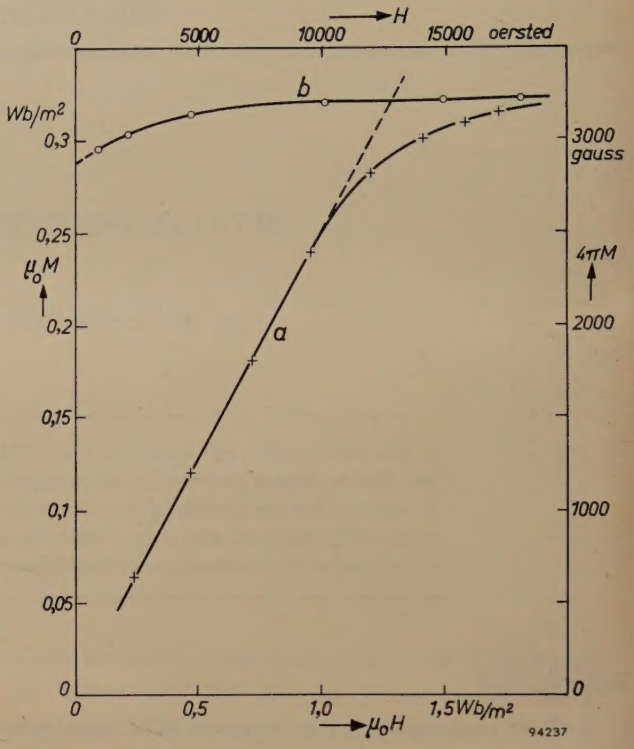

Fig. 2. The magnetization M of a Co_2Z single crystal as a function of the applied magnetic field H; *a*) preferred plane at right angles to H; *b*) preferred plane parallel to H.

the magnetization M for a single crystal of Co_2Z is plotted as a function of the applied induction $\mu_0 H$ in a direction perpendicular to the preferred plane (curve *a*) or parallel thereto (curve *b*). It can be seen from the figure that the induction $\mu_0 H$ needed to saturate the material is in the first case about 1.2 Wb/m² (field strength 12 000 oersteds), while in the second case a much smaller induction suffices for saturation.

In a normal polycrystalline specimen, the crystals have a random orientation, and therefore the specimen possesses isotropic magnetic properties. Textures are possible, however, in which anisotropic magnetic properties occur in the polycrystalline specimen. These textures are the following:

1) The basal planes of the crystals, which coincide with the preferred planes, are all parallel to one line, as illustrated in the upper half of *fig. 3a* (fan texture). In the lower half of this figure the orientation of the crystals is illustrated as they are seen when a cut is made perpendicular to the common line of the basal planes (the *c*-axes of all crystals

lie in the plane of this figure). It should be borne in mind in this connection that the crystals are generally in the form of platelets, with the smallest dimension in the direction of the *c*-axis. The permeability will now be greater in the direction of the common line than in the isotropic material, whereas the permeability in the perpendicular directions will be smaller.

2) All basal planes are mutually parallel, as illustrated in fig. 3*b* (foliate texture). In this case the permeability in all directions parallel to the basal planes is greater than that in the perpendicular direction.

As is known, the permeability is caused by the fact that an applied field $\vec{H}$ changes the direction of the spontaneous magnetization $\vec{M}_s$ in each Weiss domain if the couple $\mu_0 \vec{H} \times \vec{M}_s$ differs from zero. In ferroxplana the magnetization is so strongly bound to the preferred plane, and hence the rotation of $\vec{M}_s$ out of this plane is so slight, that this rotation makes a negligible contribution to the permeability. For this reason, the only contribution to the permeability is made by the component of $\vec{H}$ that lies in the preferred plane of a given crystal. In a specimen in which the crystals are isotropically oriented, the permeability is therefore smaller than in a specimen with aligned crystals, in which $\vec{H}$ is made to lie parallel to the preferred planes.

For the case where there is no magnetic interaction between the crystals, the alignment causes the rotational susceptibility $\chi_i = \mu_i - 1$ to increase by a factor 1.5. The interaction, however, is by no means negligible, as appears from the idealized case illustrated in *fig. 4*. This figure shows a number of crystals of a specimen, with the preferred plane of the centre crystal assumed to be parallel to the hatching and perpendicular to the plane of the drawing. The preferred planes of all the other crystals are assumed to be parallel to the plane of the drawing. In this case the lines of force of the applied field must bend to the left and right around the "crosswise" crystal, so that this crystal has a strong demagnetizing influence. As a result the permeability is smaller than that of a specimen in which the preferred planes of all crystals are in parallel alignment.

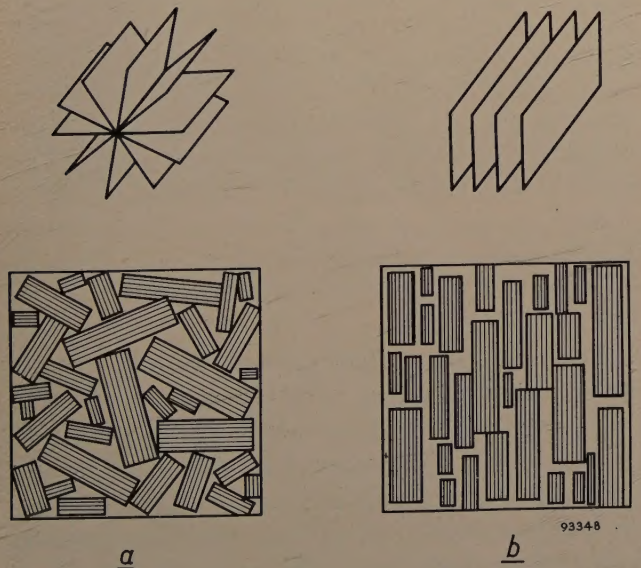

Fig. 3. Anisotropic ferroxplana. *Above*: basal planes in perspective; *below*: orientation of crystals in a section perpendicular to the basal planes. *a*) Fan texture; *b*) foliate texture.

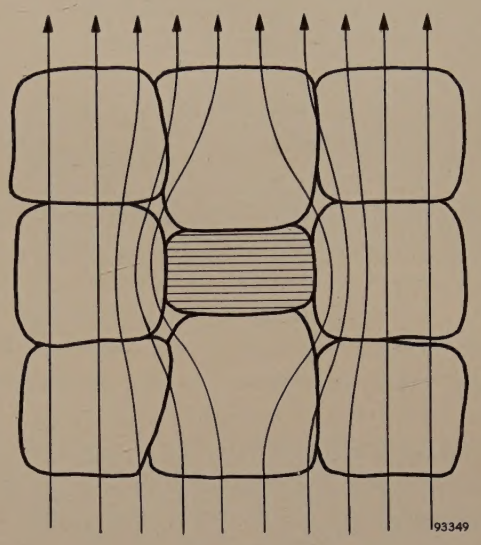

Fig. 4. Demagnetization due to a wrongly oriented crystal in ferroxplana. The preferred planes of the surrounding crystals lie in the plane of the drawing; that of the central crystal is perpendicular to the plane of the drawing and parallel to the hatching. The lines of force must bend round the "crosswise" crystal.

It will be shown below that both mechanisms here described are effective, and that therefore the permeability can be increased by the process of alignment by a factor greater than 1.5.

Methods of aligning crystals of magnetic materials

There are various known methods of producing a magnetic material with a preferred orientation.

In the case of the metallic magnetically soft materials fernicube (50Ni-50Fe) and "grain-oriented" silicon-iron (3% Si, balance Fe) a crystalline texture is obtained by rolling and subsequent recrystallization. With fernicube the preferred directions of the crystals are aligned at right angles to the direction of rolling, so that in the latter direction

the relation between the permeability and the applied field becomes more linear; with silicon-iron the permeability is increased in the direction of rolling, because the preferred directions of the crystals are aligned parallel to this direction.

Rolling cannot be applied in the same way to ceramic materials because they cannot be plastically deformed. Use might be made, however, of the special form of the particles (which, as stated, are mostly flat with the smallest dimension in the c-direction). It has been found possible with ferroxdure to obtain a crystalline texture by compressing the powdered material in a steel tube and then rolling. The effect is slight, however, and of the same order as the texture obtained by pressing the preheated powder in a die.

With some magnetically hard materials (ferroxdure, MnBi) the fact that the magnetization is strongly bound to a preferred direction can be put to very good use for aligning the crystals and thereby substantially increasing the energy product $(BH)_{max}$. (For ferroxdure, see II.) In ferroxplana the magnetization is strongly bound not to a preferred direction but to a preferred plane (as a consequence of which ferroxplana is magnetically soft). Here, too, it has been found possible to align the crystals by making use of a magnetic field. To do this we start with a uniform magnetic field $\vec{H}$ in which a number of ferroxplana crystals are placed, each of which, it is assumed, are free to rotate. The magnetization $\vec{M}_s$ of each particle is drawn in the direction of $\vec{H}$ by a couple $\mu_0 \vec{H} \times \vec{M}_s = \mu_0 H M_s \sin \alpha$ (see *fig. 5*), where α is the angle between the magnetization $\vec{M}_s$ and the field direction. The crystal anisotropy field H^A binds the spontaneous magnetization $\vec{M}_s$ to the preferred plane with a couple which proves to be equal to

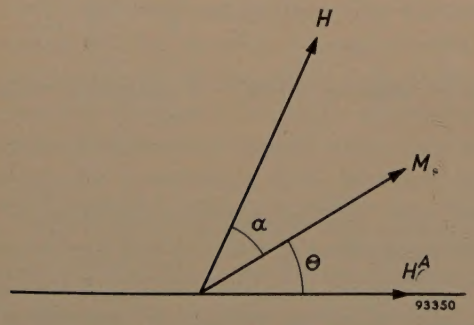

Fig. 5. Rotation of a ferroxplana crystal in an external field H. Owing to the couples $\mu_0 H M_s \sin \alpha$ and $\mu_0 H^A M_s \sin \Theta \cos \Theta$ acting on M_s, the preferred plane tends to take up a position parallel to H.

$\mu_0 \vec{H}^A \times \vec{M}_s = \mu_0 H^A M_s \sin \Theta \cos \Theta$, where Θ is the angle between the magnetization and the preferred plane. If the particle is free to move, it will then rotate until in a state of equilibrium $\alpha = \Theta = 0$, the preferred plane then being parallel to H. The plane itself can be in an arbitrary direction so that we have obtained here a fan texture.

To produce the foliate texture we subject the powder alternately to two magnetic fields whose lines of force are at right angles to each other, for example by energizing alternately two crossed electromagnets. The only stable state for the orientation of the particles is now that in which the preferred plane is parallel to both field directions, i.e. the foliate texture. Naturally, this state of equilibrium occurs only if the motion of the particles is damped, but in practice this condition is always satisfied. Instead of using two alternate, mutually perpendicular fields, we can use a magnetic field continuously varying in direction but lying in one plane, that is a rotating magnetic field which can, for example, be produced by mechanically rotating a yoke magnet. A rotating magnetic field can also be produced with a stationary magnet with the aid of the three phases of the electric mains. An electromagnet on this principle has been developed by U. Enz in the Philips Research Laboratories in Eindhoven, and has been found very suitable for alignment processes.

To produce good results a number of conditions must be fulfilled. The basic material is a magnetic powder that is obtained by pre-sintering and subsequent grinding. In the first place the preferred planes of the crystals in one particle must be mutually parallel (see II). Use is preferably made of a suspension of the powder in a liquid in order to produce a state in which the particles can readily be rotated. In order to be able to make a well finished ceramic product the particles, after orientation, should be stacked as compactly as possible. For this reason the process of aligning the particles is combined with a pressing treatment. This means, however, that the particles obstruct each other, so that an ideal state of alignment can never be achieved.

Moreover, the method can only be employed if the principal anisotropy field H^A is not too weak. For materials with a composition with which H^A is weak, as in certain mixed crystals of Co_2Z with other Me_2Z compounds, the result is therefore poor. It may be said of these materials that they show the effect typical of ferroxplana to a much lesser degree.

Fig. 6 shows two micrographs taken with an

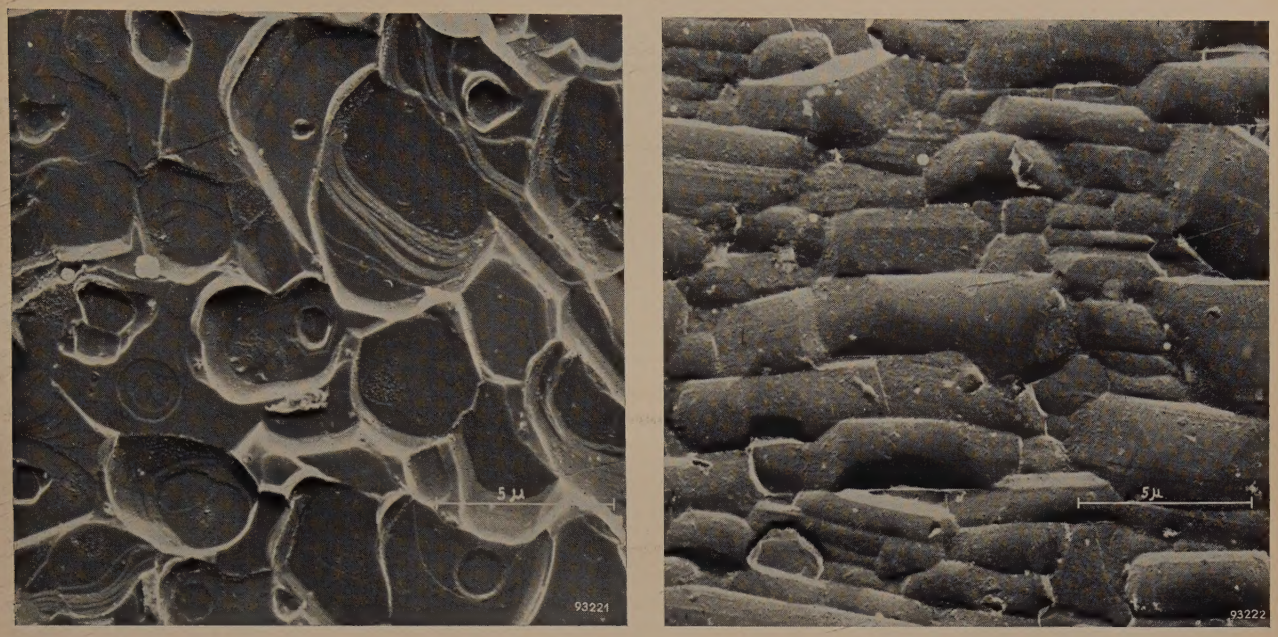

a *b*

Fig. 6. Electron-microphotographs of aligned ferroxplana with foliate texture. In (*a*) the preferred planes are parallel to the plane of the paper, in (*b*) they are perpendicular thereto.

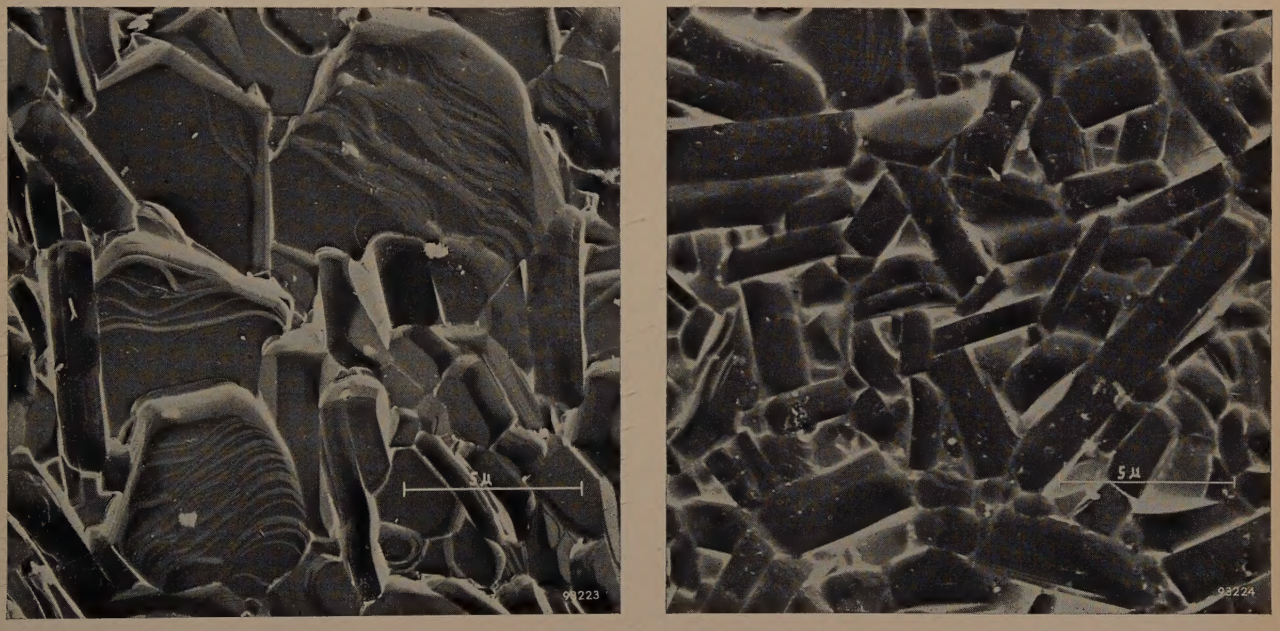

a *b*

Fig. 7. Photographs of a specimen with fan texture; the direction to which the preferred planes are parallel lies in (*a*) in the plane of the paper (roughly vertical) and in (*b*) perpendicular to the plane of the paper.

electron microscope; the foliate texture of the crystals is here clearly visible. In fig. 6*a* the preferred planes (the basal planes of the crystals) lie parallel to the plane of the paper; in fig. 6*b* they lie perpendicular thereto. The latter micrograph gives an idea of the platelet shape of the crystals. *Fig. 7* shows two micrographs of a fan texture. In fig. 7*a* the direction to which all preferred planes are parallel lies in the plane of the paper; in fig. 7*b* it is perpendicular thereto.

During sintering, anisotropic shrinkage occurs in aligned ferroxplana as it does in aligned ferroxdure. In the direction of the hexagonal axis of the crystals, the shrinkage is much greater than in the direction perpendicular thereto, as can be seen in *fig. 8*.

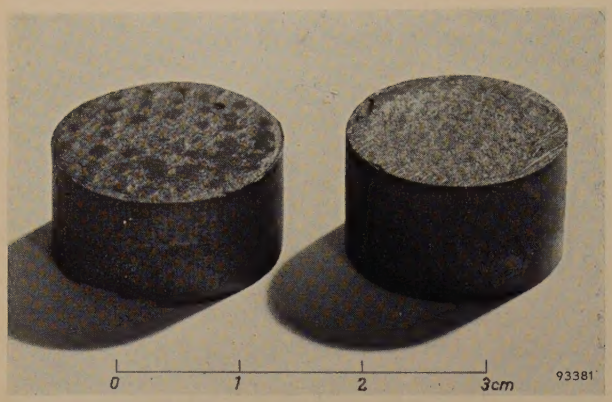

Fig. 8. Anisotropic shrinkage occurs during the sintering of an aligned pressed material. *Right:* an unaligned specimen; *left:* an aligned specimen with foliate texture. In the latter case there is considerable shrinkage in the direction of the *c*-axes of the crystals, but less at right angles to that direction. Before sintering, the dimensions of both specimens were identical.

Properties of aligned ferroxplana

The degree of alignment

The crystal-anisotropy energy in a single crystal can be found by determining the magnetization curve both in the preferred direction and in the "abhorred" direction, as in fig. 2. The anisotropy energy is equal to the area between the two curves.

For a material with a foliate texture it is possible, since the orientation of the preferred plane is known, to measure the magnetization curves in the "abhorred" direction as well as parallel to the preferred plane. If we neglect the anisotropy in the plane, we can in this way also determine the crystal-anisotropy energy for an ideally aligned material. If the material is not ideally aligned, the two curves will be closer to each other and will bound an area which is a fraction f of the area between the curves for the single crystal. We shall call this fraction f the degree of alignment of the anisotropic material. It is not possible to determine this for materials with fan texture since the preferred planes are not parallel.

The degree of alignment of specimens so treated is found to reach 90% or more.

Permeability

To ascertain how the permeability depends upon the degree of alignment, we made a number of Co_2Z specimens with foliate texture. The degree of alignment can be varied from specimen to specimen by regulating the current producing the rotating field. The density was approximately the same for all specimens. In *fig. 9* the permeability of these specimens is plotted against the corresponding degree of alignment. The figure shows clearly the considerable gain in permeability, particularly with a high degree of alignment. A compound $Co_{0.8}Zn_{1.2}Z$, which has a permeability of 22 in the unaligned state, is found to have a permeability of 55 after alignment. There are indications that, with a more complete alignment than has hitherto been possible, an even higher permeability could be obtained.

During the measurement of the permeability the applied field is naturally taken parallel to the preferred planes. If we measure at right angles to this direction, we can expect a lower permeability than in the isotropic material. In fact, a permeability of only 2.5 was measured in this way on the Co_2Z specimen with $f = 0.91$. A value of 1.3 is calculated for an ideally aligned specimen.

Apart from its greater permeability, the new material also offers advantages, owing to the anisotropic character of the permeability, when used in a magnetic circuit with an air gap. In that case the component of the stray field perpendicular to the direction of the flux will be small owing to the low permeability in this direction. A useful application that comes to mind is, for example, around the air gap of a recording head in magnetic recorders, where the stray field should be concentrated in the smallest possible space; another useful application would be for obtaining a more uniform field in an air gap.

When aligned specimens are made with a fan texture a greater permeability is found in the most favourable direction than in a corresponding unaligned specimen. The increase, however, is always smaller than in the case of a foliate texture. We assume that this is due to the fact that the degree of alignment of a fan texture will always be smaller than that of a foliate texture. In the latter we find,

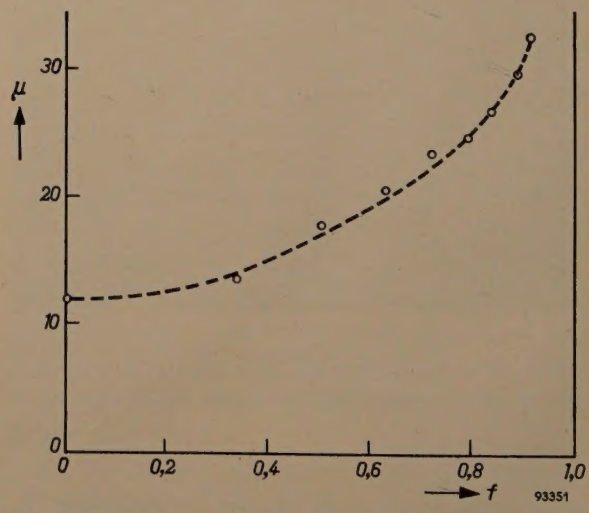

Fig. 9. The initial permeability μ of Co_2Z materials plotted against the degree of alignment f.

as in ferroxdure (see II) a marked increase in the alignment percentage during sintering at high temperature. This appears clearly from *Table I*; the degree of sintering is varied from specimen to specimen by changing the sintering temperature.

Table I. The influence of the sintering temperature on the degree of alignment f and the permeability μ of Co_2Z specimens.

Sintering temperature	f	μ
1180 °C	0.65	10.5
1200 °C	0.65	11.3
1220 °C	0.72	12.4
1240 °C	0.77	18.5
1260 °C	0.89	32.0

What probably happens is that the properly oriented crystals grow at the expense of the wrongly oriented ones, as described in II. It is not probable that the textural improvement needed for obtaining a high degree of alignment will occur in a material in which the basal planes are still in a fan-type distribution. As described, it is not possible to check this directly since f cannot be measured in a material with fan texture.

The stress anisotropy, too, can cause a difference in permeability between the materials with the two textures. Owing to the anisotropic coefficient of expansion of the crystals, more stress will arise during cooling in a material with fan texture than in one with foliate texture. If the magnetostriction is large, this is attended by a smaller permeability.

We have seen that, owing to the alignment, the permeability increases by much more than the factor of 1.5 expected for ideal alignment, owing to the fact that the external field can be applied parallel to the preferred planes. As stated, this additional gain is very probably attributable to the much smaller average internal demagnetization in aligned specimens; see fig. 4. We shall now examine this in more detail.

The internal demagnetization factor

Ferroxplana, like ferroxcube, is a sintered product containing pores. Consequently internal demagnetizing fields occur which reduce the permeability. A good impression of the demagnetization due to porosity can be obtained by measuring the so-called ideal curve. For this purpose an alternating magnetic field, whose amplitude gradually decreases from a high value to zero, is superimposed on a constant external magnetic field H. The curve which indicates the relation between the magnetization produced in this way and the intensity of the constant magnetic field is known as the ideal magnetization curve. If no demagnetization is present, the first part of the curve coincides with the magnetization axis, i.e. $(dH/dM)_{H=0} = 0$. Owing to demagnetization, the internal magnetic field H_i is not equal to the externally applied magnetic field H, and the ideal curve will make an angle α with the magnetization axis, determined by $\tan \alpha = dH/dM = N_i$, where N_i is a so-called internal demagnetization factor (see *fig. 10*). It appears thaf between N_i and the porosity p of some types to

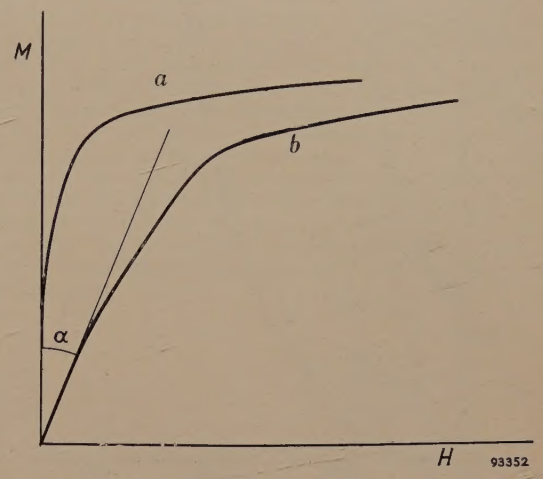

Fig. 10. The ideal magnetization curve. *a*) No internal demagnetization; *b*) internal demagnetization factor $N_i = \tan \alpha$.

ferroxcube there exists a relation as represented by the curve *a* in *fig. 11*. As long as N_i is small, μ will not be limited by the internal demagnetization but by other anisotropies; in this region, therefore, small and large permeabilities are found side by side. When N_i is large, however, the internal demagnetization prevents the permeability from reaching a high value; indeed, the values found for μ decrease monotonically with increasing N_i.

If we determine in the same way the relation between N_i and p for various unaligned ferroxplana materials we get an entirely different picture, as can be seen from curve *b* in fig. 11. Even with very dense materials a fairly large N_i factor is found which, moreover, increases rapidly with the porosity; this curve as compared with that of ferroxcube is seen to have shifted some way to the left. The corresponding permeabilities are small. This anomalous behaviour can be understood by referring to fig. 4; the crystals lying cross-wise influence the lines of force in the same way as an air pore. The demagnetizing influence is greater still: in the surrounding crystals the lines of force must continue to run parallel to the preferred plane, i.e. in the plane of the

drawing. Thus, they can only bend round to the left and right and not forwards and backwards. It is understandable, then, that the internal demagnetization in a fairly dense, unaligned ferroxplana material is just as great as in a ferroxcube material having a porosity of about 30%.

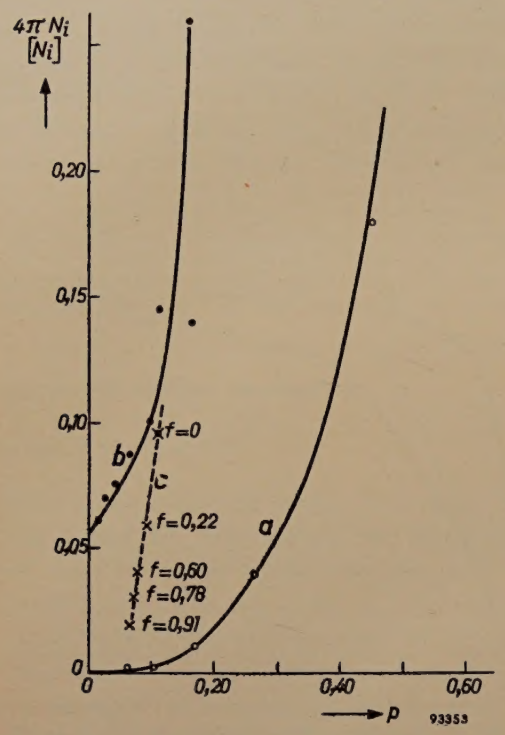

Fig. 11. The internal demagnetization factor N_i as a function of porosity p: *a*) for ferroxcube; *b*) for unaligned ferroxplana; *c*) for aligned Co_2Z with various degrees of alignment f.

We then measure N_i and p on aligned ferroxplana specimens, for which the relation between μ and f is given in fig. 9. The results of this measurement are shown in fig. 11, together with the appropriate degrees of alignment. We see that N_i decreases sharply with increasing degree of alignment f, just as expected: the ideal aligned state is approached at which, as in the case of ferroxcube materials, N_i is determined solely by the porosity. With well-aligned materials, the greatest gain in permeability is obtained by avoiding the demagnetizing influence of wrongly oriented crystals.

Frequency-dependence of the permeability

For application at very high frequencies a higher permeability is only of value if it does not entail a severe drop in the limiting frequency. In the case of specimens with a composition Co_2Z or $Co_{0.8}Zn_{1.2}Z$, therefore, the complex permeability $\mu = \mu' - j\mu''$ (μ'' is a measure of the losses: $\tan \delta = \mu''/\mu'$) was measured as a function of the frequency. The results are set out in *figs 12* and *13*; the curves for unaligned materials are shown for comparison. It is noticeable in both figures that the frequency

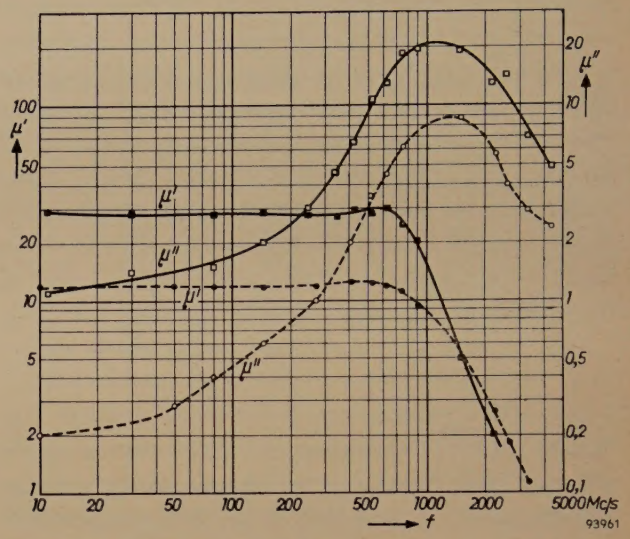

Fig. 12. The quantities μ' and μ'' as a function of frequency f; full curve for aligned Co_2Z, broken curve for unaligned Co_2Z.

at the peak of the μ'' curve is only slightly reduced by the alignment, in any case by a smaller factor than that by which the permeability is increased. The same applies to the limiting frequency f_r, if that is defined, for example, as the frequency at which $\tan \delta = 0.1$, i.e. the frequency of the point of intersection of the appertaining μ' and μ'' curves.

This can be explained as follows. Compared with an unaligned specimen an ideally aligned specimen, if the anisotropy field H_φ^A for rotations in the pre-

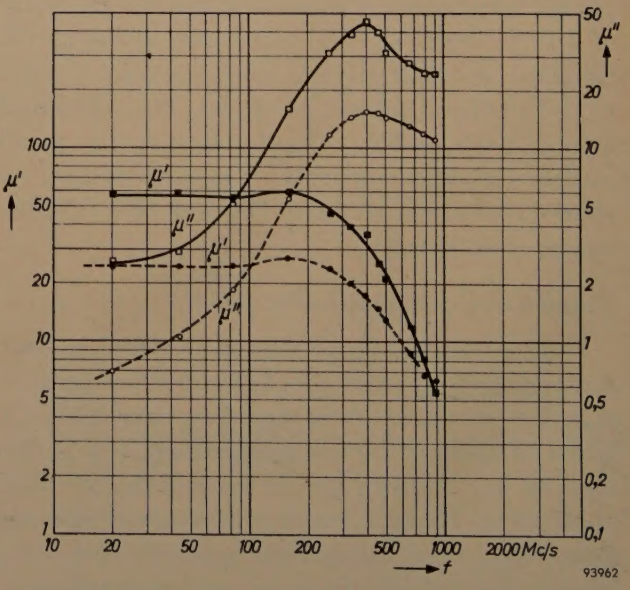

Fig. 13. The quantities μ' and μ'' as a function of frequency f for $Co_{0.8}Zn_{1.2}Z$; full curve for aligned material, broken curve for unaligned material.

ferred plane is unaltered, will show a susceptibility 1.5 times as large for a field applied parallel to the preferred plane as for a field perpendicular to this plane. As we have seen above, however, this anisotropy field H_φ^A becomes smaller by reducing the internal demagnetization; this additionally enhances the susceptibility. The large anisotropy field H_Θ^A for rotations *out of* the plane is not changed by the alignment, leaving out of account relatively small effects that might be caused by changes in the shape anisotropy. If we give all quantities of the unaligned material the suffix 1 and those of the aligned material the suffix 2, we can write:

$$\frac{\chi_2}{1.5\chi_1} = \frac{(H_\varphi^A)_1}{(H_\varphi^A)_2}.$$

From I we know that the limiting frequency f_r is proportional to $\sqrt{H_\Theta^A H_\varphi^A}$. Since $(H_\Theta^A)_1 = (H_\Theta^A)_2$, it follows that:

$$\frac{f_{r2}}{f_{r1}} = \sqrt{\frac{(H_\varphi^A)_2}{(H_\varphi^A)_1}} = \sqrt{\frac{1.5\chi_1}{\chi_2}} = \sqrt{\frac{1.5(\mu_1 - 1)}{\mu_2 - 1}}.$$

From the permeabilities μ_1 and μ_2 we calculate for Co_2Z the ratio $f_{r2}/f_{r1} = 0.77$; for $Co_{0.8}Zn_{1.2}Z$ we find $f_{r2}/f_{r1} = 0.80$. It can be seen from figs 12 and 13 that this is in good agreement with the experimental data.

Thus, by the alignment of the crystals of ferroxplana we can now obtain materials with a permeability of 30 to 50 and showing low losses up to frequencies of 200 and 100 Mc/s respectively.

Summary. Since the magnetization of ferroxplana materials is strongly bound to the preferred plane, the particles of a powdered specimen can be aligned in an external magnetic field. In a uniform field all preferred planes are parallel to the direction of the field (fan texture); in a rotating field all preferred planes are more or less mutually parallel (foliate texture). As a result the permeability becomes anisotropic and is large in certain directions; this gain in permeability is largely due to the avoidance, by alignment, of the strong demagnetizing effect of wrongly oriented crystals. In this way the permeability of some aligned specimens is increased by a factor of 2.5 to 3. For use at high frequencies it is important that the limiting frequency should not be greatly reduced; in aligned specimens this is about 0.8 times that in unaligned specimens. This effect can be explained quantitatively. The anisotropic nature of the permeability can also be put to good use in certain cases.

ANALYSIS OF THE GASEOUS CONTENTS OF SEALED CATHODE-RAY TUBES WITH THE AID OF THE OMEGATRON

544.4:621.385.832:537.534.3

Notwithstanding long and careful pumping and the use of highly active getters in cathode-ray tube manufacture, it is not feasible to evacuate below about 10^{-6} mm Hg. In addition to what is left in the tube, a certain amount of gas is liberated after the tube is sealed, both spontaneously from the various tube components and as a result of electron bombardment, from the fluorescent screen and any metal diaphragms present. The residual gas, i.e. the small fraction of the gas that is not bound by the getter, is undesirable in that it can shorten the life of the tube, *inter alia*, by poisoning the cathode [1]). If precautions are to be taken to reduce the amounts of harmful residual gases, it is necessary to know what gases are present in the tube and from which components of the tube they originate.

A useful aid to residual gas analysis has been found in the type of mass spectograph which Hipple and co-workers have called the omegatron [2]). The omegatron and cyclotron — widely different as they are in size — are analogous in that the charged particles are in both cases accelerated along (roughly) spiral paths. In the cyclotron the particles are accelerated twice per revolution in the gap between the two Dees [3]), whereas in the omegatron there is continuous acceleration in a homogeneous alternating electric field.

A schematic diagram of the omegatron is shown in *fig. 1*. A narrow beam of electrons passes from the cathode K to the electron collector A, parallel to a magnetic field of induction B. Above and below the beam, respectively, are the plates C_1 and C_2 which are connected to a radio-frequency generator G. The flat parallel rings D between these plates are so connected to tappings of a voltage divider P that there is an almost homogeneous alternating electrical field $E_0 \sin \omega t$ in the discharge space. The omegatron bulb is sealed via a glass tube to the vessel or electronic tube whose residual gas content is to be investigated.

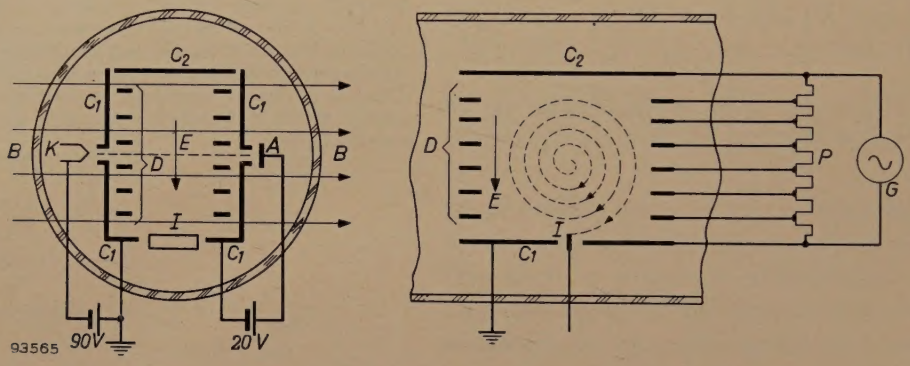

Fig. 1. Schematic diagram of an omegatron. K cathode (directly heated tungsten filament). A electron collector. C_1, C_2 plates to which the radio-frequency voltage from the generator G is applied. Flat metal rings D, connected to tappings of the voltage divider P, ensure homogeneity of the alternating electric field E in the discharge space. B constant magnetic induction. I ion collector.

The electron beam in the omegatron encounters the residual gas molecules, producing ions — almost entirely positive ions. The ions are accelerated by the R.F. field in a plane perpendicular to the magnetic field. If the angular frequency ω of the electric field satisfies the condition

$$\omega = \frac{e}{M} B \quad \ldots\ldots\ldots \quad (1)$$

(e = charge on the ion, M = mass of the ion), the resulting state of affairs is called *resonance*. This being the case, the ions describe a spiral of uniformly increasing radius (Archimedes spiral) and after making a certain number of revolutions are caught on a suitably positioned ion collector I. Ions having some other e/M ratio describe a different path and do not therefore reach the ion collector. The presence of the various ions can be successively inves-

[1]) Cf. Philips tech. Rev. **18**, 184, 1956/57 (No. 7).

[2]) H. Sommer, H. A. Thomas and J. A. Hipple, The measurement of e/M by cyclotron resonance, Phys. Rev. **82**, 697-702, 1951.

[3]) Cf. Philips tech. Rev. **12**, 67, 1950/51.

tigated by gradually varying the frequency of the electric field.

The omegatron has been used at Philips since 1953 for qualitative analysis of the residual gases in picture tubes [4]). With the type of omegatron used, it is possible with $B = 0.5$ Wb/m^2 to detect the presence of singly charged ions having a mass up to 50 (the most important residual ions have a mass in the region of 16; the heaviest are ions derived from CO_2 (mass 44) and certain hydrocarbons (masses from 44 to 58). Being of a convenient size (*fig. 2*), the omegatron can be connected by means of a short glass tube to the bulb of the picture tube before assembly; the omegatron remains connected with the picture tube while it undergoes assembly, processing and final sealing (*fig. 3*).

The other equipment is as follows. The radio-frequency voltage is drawn from a normal signal generator. The knob on the latter for adjustment of the frequency is slowly turned by a small motor so that the frequency varies through a certain range. A potentiometer, turned by the same shaft, supplies a uniformly increasing voltage; the latter is a measure of the frequency and produces a horizontal

Fig. 2. One of the omegatrons employed.

Fig. 3. An omegatron *O* connected to a picture tube *C* between the poles of a permanent magnet *M* which provides the constant magnetic field.

[4]) Before this article went to press a paper on the same subject appeared elsewhere, namely: J. S. Wagener and P. T. Marth, Analysis of gases at very low pressures by using the omegatron spectrometer, J. appl. Phys. **28**, 1027-1030, 1957 (No. 9). The results reported agree broadly with those presented here.

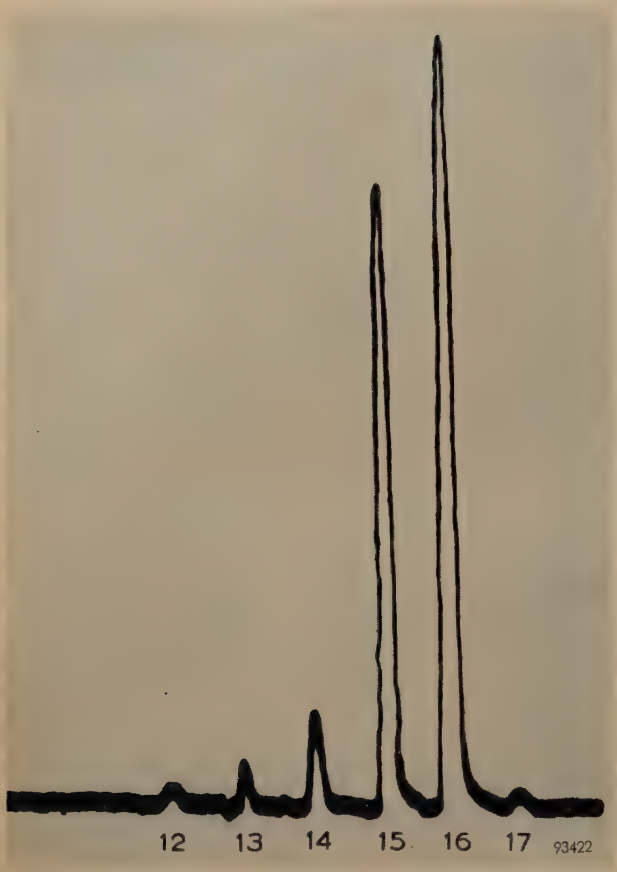

Fig. 4. A typical spectrogram. The peaks occur at frequencies which correspond, according to (1), to $M = 12, 13, 14, 15, 16$ and 17 (the ions carrying a single elementary charge e); these peaks are almost entirely attributable to C^+, CH^+, CH_2^+, CH_3^+, CH_4^+ and $C^{13}H_4^+$, respectively.

deflection on a cathode-ray oscilloscope. The current from the ion collector passes through a 10^{11} ohm resistor and the voltage across this resistor is amplified to give the vertical deflection. The light spot on the oscilloscope describes a curve which exhibits a peak at each frequency, the position of which, according to (1), corresponds to the mass M of the ions present. At present the heights of the pulses do not give an accurate measure of their relative concentration.

Some results of the investigation are given below. The principal residual gases that have been found in picture tubes are:

1) Methane. This gas was encountered in all the tubes examined. The high peak at $M = 16$ in the spectrogram (*fig. 4*) stems from CH_4^+ ions; the lower peaks at $M = 15$, 14, 13, 12 correspond to CH_4 fragments, viz. the ions CH_3^+, CH_2^+, CH^+ and C^+, respectively. The peak at $M = 17$ can be attributed to CH_4^+ with the carbon isotope C^{13}. The methane pressure falls with the passage of electrons in the picture tube, but rises again somewhat during periods of rest.
2) Argon. This gas was also found in all the tubes examined, but only after vaporization of the getter.
3) The various other residual gases met with depend upon the way in which the tube is manufactured and the materials used. The most common are hydrogen, carbon monoxide, carbon dioxide and hydrocarbons other than CH_4.

An example of a case in which CO and CO_2 can be expected are tubes in which the fluorescent screen is covered with a thin aluminium reflector ("metal backing") serving to reflect inwardly-radiated fluorescent light from the screen. If, deliberately, too little barium getter is vaporized in such a tube, there will be a rise in pressure subsequently when the tube is in use; this is brought about by CO and (to a lesser extent) by CO_2. These gases are in this case probably mainly produced when electrons collide with minute residual traces of the nitrocellulose film (the latter forms the underlayer for the aluminium and is removed by baking when it has served its purpose [5]).

Work is in progress with a view to making the omegatron and its associated apparatus suitable for quantitative analysis.

J. PEPER.

[5]) J. de Gier, Philips tech. Rev. **10**, 102, 1948/49.

A SIMPLE APPARATUS FOR CONTACT MICRORADIOGRAPHY BETWEEN 1.5 AND 5 kV

by B. COMBÉE and A. RECOURT.

778.33:621.386.1

Microradiography, the X-ray photography of microscopic specimens, can provide important information, unobtainable with an optical microscope. In principle, it is a fairly old technique, but its intricacy has hitherto debarred it from extensive use in hospitals and biological laboratories. With the appearance of the apparatus described in this article, the CMR 5, which is equipped with a small, sealed-off X-ray tube having a beryllium window only 50 microns thick, microradiography has now come within the range of every biologist or medical worker, and may even be employed for routine pathological examinations. The article below, after an introductory discussion of microradiography in general, describes the construction and uses of this new instrument. It appears that the resolution, which is now determined by the film, is 0.5 to 1 micron and hence not far behind what can be achieved visually with an optical microscope (about 0.3 micron).

Introduction

Among the methods of microscopic investigation, microradiography is rapidly gaining in significance and now occupies an important position along with optical and electron microscopy. In microradiography a radiograph is made by the "normal" method of shadow projection, and the X-ray image so obtained is examined with a magnifying glass or under a microscope. Thus it is not, as might at first be thought, microscopy with X-rays [1]), and therefore as regards resolution, the method does not offer the advantages that might be obtained with the very short wavelengths of an actual X-ray microscope [2]).

The fact that microradiography is nevertheless of great significance is due in the first place to the ability of X-rays to penetrate objects which are not transparent to light and electrons. Moreover, with our knowledge of the absorption of X-rays by matter, we can learn from a radiograph not merely the geometry of the object, but also something of its chemical composition. For example, it has proved possible in this way to determine the weight of histological and cytological [3]) structures and to carry out quantitative chemical analyses. Finally, by analogy with the staining of specimens for examination under an optical microscope, good use can be made of X-ray contrast media, which again offer quite different possibilities.

Before dealing with the apparatus which is the subject of this article, we shall examine briefly the laws governing the absorption of X-rays and the methods of projecting an X-ray shadow image on a film.

The absorption of X-rays; contrast

The attenuation which a parallel beam of monochromatic X-rays undergoes in matter is given by the formula:

$$I = I_0 \, e^{-\mu d}, \quad \ldots\ldots\ldots \quad (1)$$

in which I_0 is the initial intensity, I the intensity when the beam has traversed a layer of material of thickness d, and μ is the absorption coefficient. The way in which μ varies with the wavelength λ of the radiation and with the atomic number Z of the elements of which the absorbent material is composed is given for a wide range of wavelengths by the formula:

$$\mu = C\lambda^3 Z^4, \quad \ldots\ldots\ldots \quad (2)$$

in which C is a constant.

The dependence on λ is demonstrated in *fig. 1a*, which shows by how much an X-ray beam is attenu-

[1]) Although advances have been made in this field in recent years, the experimental X-ray microscopes so far developed are no better than optical microscopes as far as their resolving power is concerned. As regards magnification and field of view, they are greatly inferior. See P. Kirkpatrick and A. V. Baez, J. Opt. Soc. Amer. **38**, 766-774, 1948 and P. Kirkpatrick and H. H. Pattee, Advances biol. med. Phys. **3**, 247-283, 1953.
See also for X-ray optics: Y. Cauchois, Rev. Opt. **29**, 151-163, 1950 and M. Montel, Rev. Opt. **32**, 585-600, 1953; Optica Acta **1**, 117-126, 1954; C. R. Acad. Sci. Paris **239**, 39-41, 1954.

[2]) For a discussion of the dependence of the resolving power of microscopes on the wavelength of the light used, see, e.g., J. B. le Poole, Philips tech. Rev. **9**, 33-45, 1947/48.

[3]) *Histology* is the study of the structure of tissues, *cytology* the study of the structure of cells. Cells are the units of which tissues are composed.

ated in a layer of animal tissue 10 microns thick, in a 1 cm layer of air and in a layer of beryllium 50 microns thick; at a wavelength of 2 Å these layers are almost entirely transparent, whereas at 15 Å they absorb nearly all the radiation. Curves *2* and *3* of this figure reveal something of the very pronounced influence of Z. The atomic number of beryllium is 4, while the effective atomic number of air lies between 7 (nitrogen) and 8 (oxygen). If the layer of air were to be compressed to the density of beryllium, it would be only 7 microns thick, and yet it absorbs almost as strongly as the seven times thicker layer of beryllium.

The curve that represents absorption (or transmission) as a function of wavelength does not always have the continuous form shown in fig. 1*a*. In fig. 1*b* we see the absorption in a layer of photographic emulsion 5 microns thick plotted against the same range of wavelengths. At 3.7 and 7.0 Å there are abrupt discontinuities in the curve; these absorption edges, as they are called, occur at wavelengths which are characteristic of every element, and are caused here by silver and bromine.

At the wavelengths with which we are concerned, the attenuation of the X-ray beam is chiefly caused by the photo-electric effect. Where λ is large, electrons are liberated only from the outermost shell or shells of the atoms of the absorbent substance. As λ decreases, however, (i.e. as the energy of the X-ray quanta increases) a limit is reached where electrons can be liberated from the next, deeper shell, and the absorption suddenly becomes greater. These sharp discontinuities in the absorption curve are the above-mentioned absorption edges. They are denoted by the letter of the electron shell concerned, i.e. as K, L, M etc. (starting from the innermost shell of the atom). The curve in fig. 1*b* shows the L absorption edges of bromine and silver. The absorption edges of the elements making up the substances represented in fig. 1a lie at wavelengths longer than 15 Å.

Fig. 1*b* again illustrates the pronounced increase of absorption with atomic number. Although the emulsion layer is only 5 microns thick and only a small part of its volume consists of AgBr, the contributions of Ag and Br are nevertheless so substantial that the layer absorbs nearly as strongly as the layers of fig. 1*a*, and even more strongly below 3.7 Å.

While the great penetrating power of X-radiation is one of the fundamentals of microradiography, it is also necessary, of course, that the different parts of an object should exhibit distinctly different degrees of transparency, that is to say the rays must be differentially absorbed by the object. In view of the extreme thinness of the specimens (10-100 microns) this means that μ must be high. From equation (2) it is immediately apparent that soft X-radiation is required to get a large value of μ, although the gain in contrast must be paid for by a longer exposure.

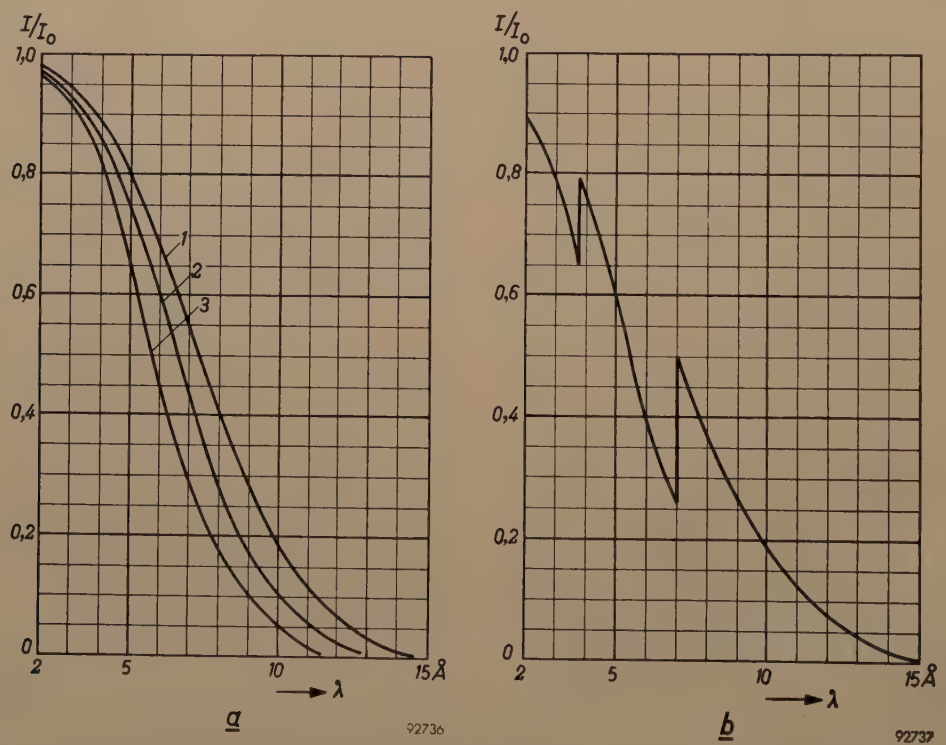

Fig. 1. *a*) Relation between the intensity of transmitted and incident X-radiation as a function of the wavelength, for three different absorbent layers:
1 animal tissue 10 microns thick, *2* layer of air 1 cm thick, and *3* beryllium foil 50 microns thick.
b) The same for the 5 μ thick emulsion layer of Kodak "Maximum Resolution" film. The discontinuities in the curve are the L absorption edges of bromine (left) and silver (right).

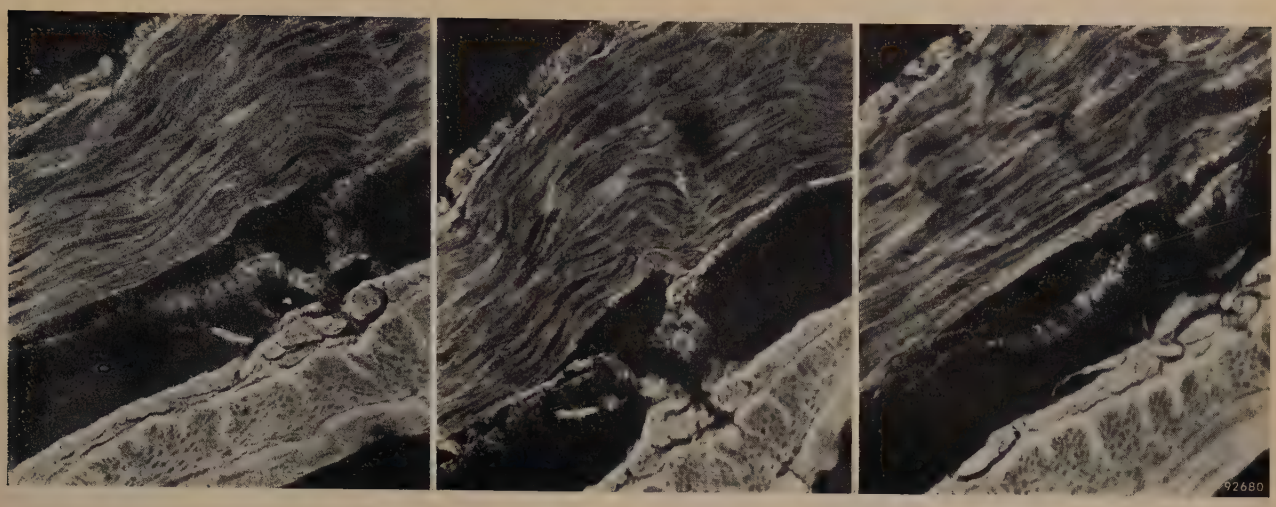

Fig. 2. Section of the oesophagus of a guinea pig (cavia). The light part is the mucosa (a glandular layer) on the inner oesophagal wall. The micrographs, from left to right, were taken at anode voltages of 5, 3 and 1.5 kV respectively, on Kodak "Spectroscopic" film 649-0. As can be seen, the contrast changes with the anode voltage. Magnification 130×.

It may be deduced that the film will show maximum contrast between two parts of an object with only slightly differing values of μ if the product μd is approximately equal to unity [4]). If we have a section of 20 microns thickness, i.e. 2×10^{-3} cm, then μ must be about 500 cm^{-1} in order that μd be equal to unity. For soft, animal tissue consisting of, say, 25% dry matter, this is the case when $\lambda = 11$ Å; for hard tissue (bone) the optimum wavelength with the same specimen thickness is 3 to 4 times shorter. Fortunately, however, fairly wide deviations from these optimum conditions cause no serious loss of contrast. The three micrographs in *fig. 2*, representing a cross-section of the oesophagus of a cavia (guinea pig), illustrate how the contrast changes as the X-radiation is made softer.

Projection microradiography and contact microradiography

A radiograph can be taken either by bringing the object and the film into close contact or by placing the film at some distance behind the object. In the first case the X-ray image is as sharp as it can be; in the second case there is some magnification, the X-ray image being larger than the object owing to projection (projection radiography [5])). The drawback of projection is that it gives rise to a penumbra (geometric unsharpness), the width of which increases with increasing distance between object and film. This phenomenon is illustrated in *fig. 3*.

It can be seen that the geometric unsharpness O_g may be expressed by the formula:

$$O_g = \frac{f\,b}{a-b}, \quad \ldots\ldots \quad (3a)$$

where f is the size of the tube focus and a and b are the distances between focus and film and object and film, respectively. By introducing the magnification V, equal to $a/(a-b)$, we may write

$$O_g = (V-1)f. \quad \ldots\ldots \quad (3b)$$

If object and film are in contact, O_g is very small, since in that case $b \approx 0$ or $V \approx 1$.

To determine the resolution obtainable, O_g should be compared with the linear dimensions of the *image*, which means that the linear dimensions of the

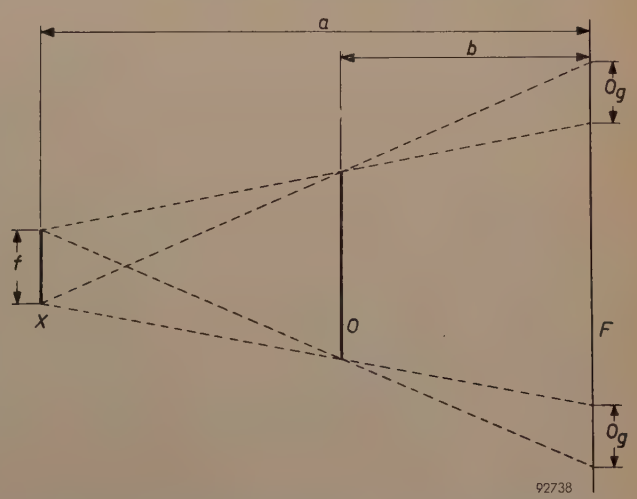

Fig. 3. The geometric unsharpness O_g of a microradiograph is determined by the dimensions of the focus (X) and the distances from film (F) to focus and from film to object (O). If the latter distance is very small (contact method), O_g is also very small.

[4]) A. Engström and R. C. Greulich, J. appl. Phys. **27**, 758-759, 1956.

[5]) See e.g. M. von Ardenne, Elektronen-Übermikroskopie, Springer, Berlin 1940, p. 72, and V. E. Cosslett and W. C. Nixon, Proc. Roy. Soc. **B 140**, 422-431, 1952.

object must be compared with O_g/V. With formula (3b) the resolution is then found to be

$$\frac{O_g}{V} = \frac{V-1}{V} f. \quad . \quad . \quad . \quad . \quad . \quad (4)$$

This, then, is the smallest spacing there can be between two object details without their penumbrae overlapping, i.e. the smallest dimension a detail may have in order for its umbra still to reach the film. Expression (4) becomes very small when V approaches 1. At large V the resolution is practically equal to the diameter of the focus [6]).

To demonstrate this we shall take a numerical example. If the thickness of the object is 10 microns and that of the sensitive layer 5 microns, then b (formula 3a) in the case of contact is at the most 15 microns. Where the focus-film distance is 15 mm and the diameter of the focus 0.3 mm (300 microns), it follows from formula (3a) that O_g is at the most 0.3 micron. If, however, other conditions being equal, we take a projection radiograph with $b = 7.5$ mm, then $O_g = 300$ microns and, since $V = 2$, the smallest spacing separately distinguishable in the object is 150 microns.

Nevertheless, the above does not permit the conclusion that contact microradiography always produces better resolution than projection microradiography, for we have not yet taken the properties of the film into account. Owing to the fact that the sensitive layer is not a continuum but a suspension of light-sensitive AgBr grains in gelatine, the film itself has a limited resolving power. Let K be the smallest spacing that the film can resolve, then it is obvious that nothing more can be gained when $f(V-1)/V$ becomes smaller than K. With a very fine focus this limit is reached at a magnification considerably greater than 1. Thus, the spacing between two details which can be resolved, K/V, is thus in this case smaller than K, the threshold value in contact microradiography. If, for example, $f = K$, the optimum enlargement is $V = 2$ and the smallest distinguishable spacing is $K/2$.

The instrumental complications involved in the use of such an extremely fine focus, and the fairly low intensity of such an X-ray source, make the contact method preferable for many purposes, the more as it becomes possible to produce films with a smaller K. Moreover, the minimum tube voltage for projection microradiography is appreciably higher, owing to the necessity of using a transmission target [5]). In the following pages, therefore, we shall be concerned solely with contact microradiography.

The CMR 5 apparatus for contact microradiography

The necessity of using very soft X-rays has hitherto further complicated the technique of microradiography, since it was not possible to make sealed-off X-ray tubes with windows that would let through enough of the radiation required. Windows of sufficiently thin light-metal foil, such as beryllium and aluminium, were not vacuum-tight and the tubes employed had therefore to be continuously evacuated.

In recent years, however, it has proved possible to make vacuum-tight windows of beryllium foil only 50 microns thick. Because of the low atomic number of beryllium (4) the X-ray absorption in these windows is sufficiently small for the purposes of microradiography (see fig. 1*a*, curve 3). An X-ray tube for microradiography equipped with such a window, and intended for anode voltages from 1.5 to 5 kV, is shown in *fig. 4*. A photograph of this tube is shown in *fig. 5*. The dimensions of the focus are 0.3×0.3 mm, and the focus-to-window distance is 11 mm. The fine focal spot is obtained by electrostatically focussing the electron beam, use being made of a cathode construction which has been

[6]) In accordance with the usage in microscopy, the term "resolution" denotes here the spacing between two details or objects that can just be separately distinguished.

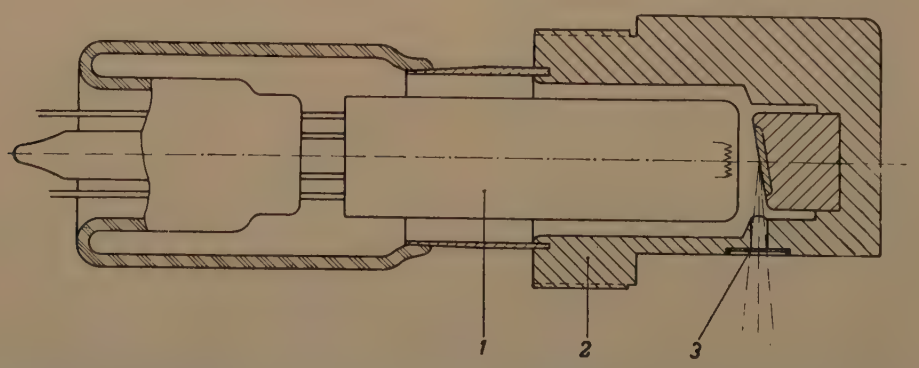

Fig. 4. Cross-section of X-ray tube for microradiography between 1.5 and 5 kV. *1* cathode with tungsten filament; *2* anode with tungsten target; *3* beryllium window 50 microns thick. The tube is 8 cm long. The (effective) size of the focal spot is 0.3×0.3 mm.

employed for some time now in fine-focus tubes for X-ray diagnostic technique [7]).

Fig. 6 shows a photograph of the CMR 5 apparatus in which the X-ray tube described is incorporated. The tube is mounted in the protruding section on the right, the window being underneath.

The apparatus contains the power supply circuit for the tube, the anode voltage being continuously variable. There is also a control for varying the tube current, so as to prevent over-loading of the tube (maximum power 10 W). The filament current is stabilized by means of a current stabilizer tube. The anode voltage and tube current can be read from meters on the front panel. After the controls have been set at the required values, the anode voltage can be switched off (in order, for instance, to load and mount the film-holder) without at the same time switching off the filament current, although the latter is then automatically somewhat lowered with a view to prolonging the life of the tube. In this way, steady operating conditions are rapidly reached when the

Fig. 5. Photograph of the X-ray tube shown in fig. 4.

[7]) See G. C. E. Burger, B. Combée and J. H. van der Tuuk, Philips tech. Rev. **8**, 327, 1946.

Fig. 6. The CMR 5 apparatus for contact microradiography. On the front panel can be seen the meters and controls for tube current (max. 5 mA) and anode voltage (max. 5 kV). The knob in the middle is used for fine adjustment of the current. The pilot lamp on the left is lit when the H.T. is on. The dial illumination lamp between the meters is switched on with the switch marked *L*. The other two switches are for mains and H.T. The X-ray tube is mounted inside the projecting section on the right of the case. The film-holder is inserted in the cylindrical container underneath the tube (see fig. 7).

high tension is switched on, so that it is not usually necessary to take warming-up into account when deciding exposure times.

The film-holder is mounted in the vertical cylindrical container under the X-ray tube. *Fig. 7* illustrates how this container is fixed to the X-ray

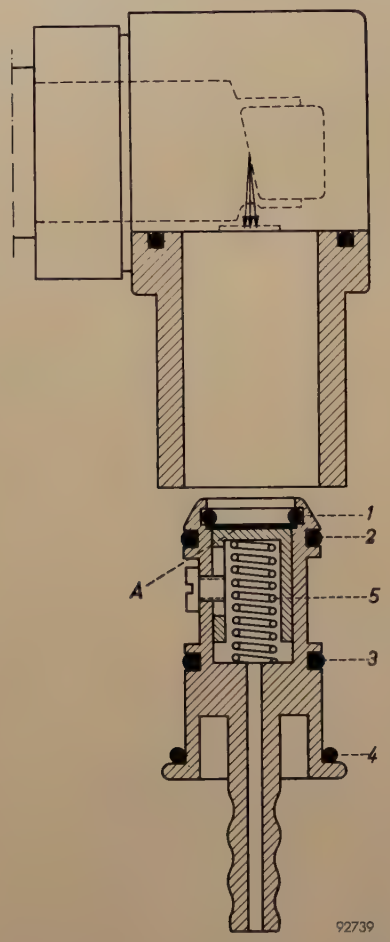

Fig. 7. The target end of the X-ray tube, showing attached cylinder into which the film-holder is inserted. Underneath is the film-holder itself, loaded with film, specimen and specimen carrier. The pressure plate is in the form of a plunger which, under the action of a spring *5*, keeps the film, specimen and specimen carrier (*A*) pressed against a rubber ring *1*. The other rubber rings (*2*, *3* and *4*) ensure a good seal, making it possible to evacuate the film-holder by attaching a vacuum line (a water-jet pump provides sufficient vacuum) to the nozzle provided for the purpose.

tube and shows a cross-section of the film-holder. In effect the film-holder is simply a cylinder with a spring-loaded plunger inside it; the plunger ensures that film, specimen and specimen base are kept pressed against the rubber ring *1*.

As can be seen in figs 6 and 7, the film-holder is provided with a nozzle, to which a vacuum-hose (connected, say, to a water-jet pump) can be fixed for the purpose of partially evacuating the film-holder and so reducing practically to zero the absorption in air which, as fig. 1*a* shows, cannot be left out of account.

For exposures longer than about 15 minutes, it is desirable to cool the X-ray tube; this can be done by connecting a fan to a point at the rear of the apparatus, the air then being drawn in through perforations in the protective shield around the end of the X-ray tube. This keeps down the temperature of film and object and prevents unsharpness arising from the mutual displacement of object and film due to thermal expansion.

Quality of the X-radiation

When applying the laws governing the absorption of X-rays in matter it should be borne in mind that the radiation generated in the apparatus and used for making the micrographs has a continuous spectrum. Ignoring the characteristic radiation also emitted, we can express the form of this spectrum by the equation [8]):

$$I(\lambda) \propto \frac{1}{\lambda^2}\left(\frac{1}{\lambda_0}-\frac{1}{\lambda}\right), \quad \ldots \quad (5)$$

where $I(\lambda)$ is the intensity of the radiation at a wavelength λ, and λ_0 is the shortest wavelength of the spectrum. Between the latter wavelength (in Å) and the anode voltage of the X-ray tube (in kV) there exists the relation:

$$\lambda_0 = \frac{12.39}{V}. \quad \ldots \ldots \quad (6)$$

Curve *1* in *fig. 8* shows the form of the spectrum after the radiation has passed through the beryllium window, the anode voltage being $V = 3$ kV. The minimum wavelength is 4.11 Å, but the maximum intensity occurs at 6 to 7 Å. It appears, then, that V must be made about $1^1/_2$ times larger than corresponds to the wavelength demanded by considerations of contrast and exposure time. The other curves in this figure show how the intensity is diminished after the rays have passed through a layer of tissue 10 microns thick and through the same layer plus the 5 micron thick emulsion of a Kodak "Maximum Resolution" film.

The film; magnification of the micrographs

Since there is very little geometric unsharpness in contact microradiography, provided the objects are sufficiently thin, the resolution obtainable is determined by the resolution of the film. The films most suitable for the purpose are Gevaert "Lippmann", Agfa "Mikrat", Eastman-Kodak "649-0" and Kodak "Maximum Resolution". These films have a resolving

[8]) H. A. Kramers, Phil. Mag. (6) **46**, 836-871, 1923. R. H. de Waard, Acta radiol. **28**, 37-48, 1947.

power of approximately 1000 lines per millimetre. Compared with most other films this figure is exceptionally high, but for microradiography an even higher figure would be desirable. The AgBr grains of the last mentioned film, for example, which have a diameter of about 0.045 micron, fill only a fraction of the total volume; there are some 200 grains per cubic micron and therefore about 6 per linear micron. Moreover, the grains are distributed not in perfect uniformity but at random. Obviously, in the image formed on such an emulsion it will be impossible to distinguish between details that are very much smaller than one micron, especially since a developed film, when viewed through a microscope, reveals a mottled structure of silver "grains" which consist of aggregates of the silver particles produced from the individual AgBr crystals during photographic development. It is this "graininess" that determines the resolution which the emulsion will give, it being understood, of course, that the resolution can never be better than the grain density of the original AgBr crystals permits.

In practice one can reckon on a resolution of 0.5 to 1 micron, which is almost as good as that obtainable visually with optical microscopes (0.3 micron). The micrographs can therefore be examined under a normal microscope with a magnification of, for example, 500×.

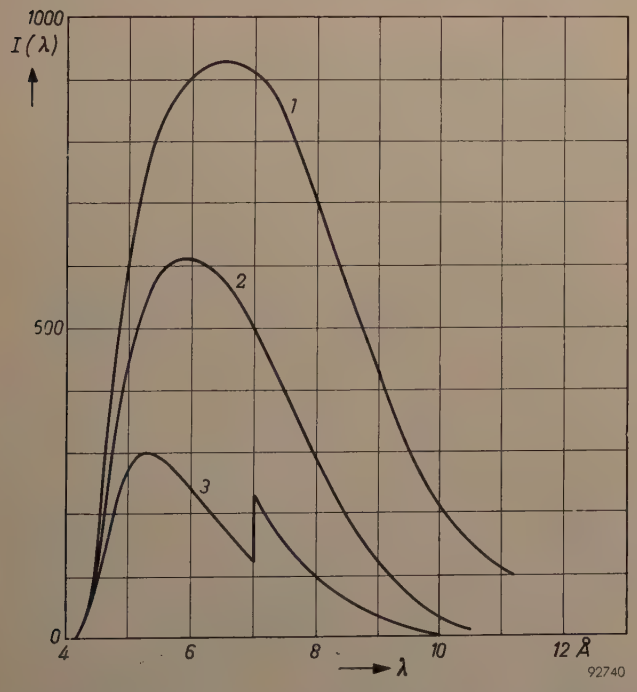

Fig. 8. Curve *1* shows the intensity distribution of the continuous spectrum of X-radiation generated in the CRM 5 apparatus at an anode voltage of 3 kV, and measured just outside the beryllium window. Curve *2* represents the spectral distribution of this radiation after it has passed through a layer of animal tissue 10 microns thick, and curve *3* after it has in addition traversed a 5-micron layer of emulsion on Kodak "Maximum Resolution" film. The discontinuity in the latter curve is due to the L absorption edge of silver.

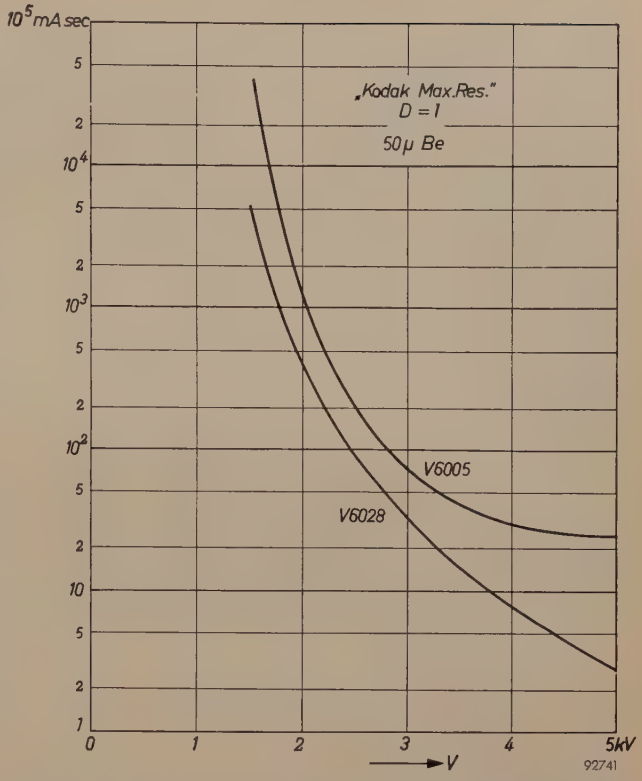

Fig. 9. The exposure, expressed in mA.sec, needed to produce a photographic density 1, as a function of anode voltage. The upper curve relates to standard Kodak "Maximum Resolution" film (emulsion V 6005) and the lower to an experimental Kodak emulsion V 6028. The curves show that the latter emulsion is at least 2× as sensitive as the other, and at 5 kV even 10× as sensitive.

The ideal emulsion for microradiography should have about the same absorption as the above, but should have a greater grain density and above all less graininess. Several film manufacturers have been attempting to produce emulsions with these properties, but their efforts have led rather to films of greater *sensitivity* — which is also an important point — than to films of higher resolving power.

This is illustrated in *figs 9*, *10* and *11*, which relate to an experimental emulsion V 6028 by Kodak [9]). The experimental emulsion differs from the standard "Maximum Resolution" emulsion (type V 6005) in that it is only 1 micron thick instead of 5, and has 100 times more grains per unit volume; the size of the AgBr grains is the same. The curves in fig. 9 show what exposure, expressed as the product of tube current (mA) and time (seconds) is needed at a given anode voltage in order to produce a photographic density $D = 1$. The graph shows that the new emulsion is 2 to 10 times as sensitive as the old

[9]) We are indebted to Dr. R. W. Berriman and Dr. R. H. Herz (Research Laboratory Kodak Ltd.) for preparing this emulsion and placing it at our disposal.

Fig. 10. Comparison of the graininess of standard emulsion V 6005 (above) and experimental emulsion V 6028, each with the same photographic density. Both exposures were made at an anode voltage of 3 kV. It can be seen that the new emulsion has about the same graininess as the old. Magnification 1200×.

one. Fig. 10 gives an impression of the graininess of the two emulsions with identical photographic density, and fig. 11 allows a comparison of the resolution in each case. The photographs show that the graininess of the new emulsion is neither more nor appreciably less pronounced than that of the other emulsion. It can be said, then, that the experimental emulsion V 6028 is much more sensitive than the "Maximum Resolution" type hitherto in use, without there being any decline in its resolving power.

It has been noticed that the resolving power of an emulsion is greater the softer the X-radiation employed. Experiments have shown that at anode voltages less than 1 kV it is possible to distinguish on one of the above-mentioned films details as small as 0.2 micron. In that case, magnification by an optical microscope is no longer adequate and an electron microscope must be used instead. We shall return to this subject presently.

Applications

Microradiography is used most for biological and medical research, particularly in the fields of histology and pathological anatomy. In these fields the technique can be put to the following uses to provide information unobtainable by optical microscopy.

a) Examination of opaque objects (e.g. bone tissue).

b) Examination of transparent objects, parts of which become visible because their chemical com-

Fig. 11. Comparison of the resolution of emulsion V 6005 (above) and emulsion V 6028 (below). The two micrographs on the left were taken at an anode voltage of 3 kV, the two on the right at 1.5 kV. The object radiographed was a fine silver mesh, the thicker wires being 6 microns in diameter, the thinner 2 microns. It can be seen that the resolution of the experimental emulsion is roughly equal to that of the old; at 1.5 kV it is perhaps slightly better.

position differs substantially from that of their environment, or can be made visible by contrast media; this is especially important with regard to parts that are not easy to find with the aid of the dyes commonly used in optical microscopy.

c) Determination of the (dry) weight per unit area of an object, or detail, of known chemical composition, from the degree of X-ray absorption.

d) The performance of localized quantitative chemical analyses when the composition is known qualitatively.

In the following we shall briefly discuss, or exemplify, the four applications mentioned [10]). Before doing so, however, we shall give a synopsis of the technique employed in optical microscopy for preparing specimens of biological objects, and consider what parts of this technique can be adopted, omitted or modified for preparing specimens for microradiographic examination.

Preparation of specimens [11])

The procedure for preparing specimens for examination with an optical microscope is carried out in the following six stages:

1) *Fixation.* When a fragment is removed from a living object, that fragment slowly dies and thereby undergoes all manner of changes. To prevent such degeneration, the fragment is quickly immersed in a fluid which rapidly penetrates and kills the tissues and so fixes the fragment in as life-like a state as possible. Depending upon the object, the fixing fluids employed include alcohol (96%), acetic acid, formalin and osmium tetroxide (OsO_4), sometimes referred to as osmic acid.

2) *Embedding.* In order to be able to cut the fixed fragment into sufficiently thin sections, it is necessary, as a rule, to embed it in (i.e. thoroughly impregnate it with) a hardener such as paraffin wax. For this purpose the fragment is first dehydrated by immersing it in increasingly concentrated solutions of alcohol in water (in about ten stages). After that it is immersed (in three stages) in solutions of alcohol and xylol, the xylol content being increased at each stage, and finally, via a solution of paraffin wax in xylol, embedded in pure paraffin wax.

3) *Sectioning.* The embedded fragment is cut into thin sections with a microtome.

4) *Attaching specimen to slide.* This is done by applying first a drop of protein-glycerine to the slide, and then a drop of distilled water, taking care that it spreads well over the glass surface. The specimen is now placed on the slide and gently warmed (without melting the paraffin wax) until it lies flat. Finally, the water is drained off and the specimen left to dry in air, after which it is treated with xylol to remove the paraffin wax.

5) *Staining.* After the paraffin wax is removed, the procedure mentioned under 2) is reversed to return to the hydrated state. It is then possible to stain the specimen. The choice of stain depends on what detail one wishes to see. Among the frequently used stains are such synthetic dyes as methyl-blue, fuchsin, eosin (for staining the plasma), and natural dyes such as hematoxylin (for staining cell nuclei).

6) *Mounting.* The specimen is finally rinsed with alcohol and xylol and mounted in Canada balsam after which a cover-glass is placed over it.

For radiographic examinations the procedure is the same as described in 1) to 3) above. After that, however, the specimen is not mounted on a slide but on a formvar film stretched across a metal ring. Since formvar is resistant to xylol, the paraffin wax can be removed by the normal process [12]). No staining is involved, although a contrast medium may be applied where necessary. The mounting procedure under 6) is, of course, also irrelevant here.

For some purposes where the requirements are not so strict, the preparation of the specimens can be simplified. For example, the fixation and embedding procedures can be replaced by freezing, a special microtome then being used for sectioning. In this way the time spent on specimen preparation can be reduced from 1 or 2 days to 1 or 2 hours.

Examination of opaque objects

The advantage of contact microradiography over optical microscopy is obvious in the examination of opaque objects. *Fig. 12* shows a micrograph of bone tissue. Around the blood vessel the density is appreciably greater (i.e. there is less X-ray absorption) than at some distance away.

[10]) The latter two fields are dealt with comprehensively in an article by A. Engström, Historadiography, in Physical techniques in biological research Vol. 3, Acad. Press, New York 1956.

[11]) For a full treatment of this subject, see e.g. P. Metzner-A. Zimmermann, Das Mikroskop, F. Deuticke, Leipzig and Vienna 1928.

[12]) The formvar film (polyvinylformaldehyde) is only a few tenths of a micron thick and absorbs X-radiation only very slightly.

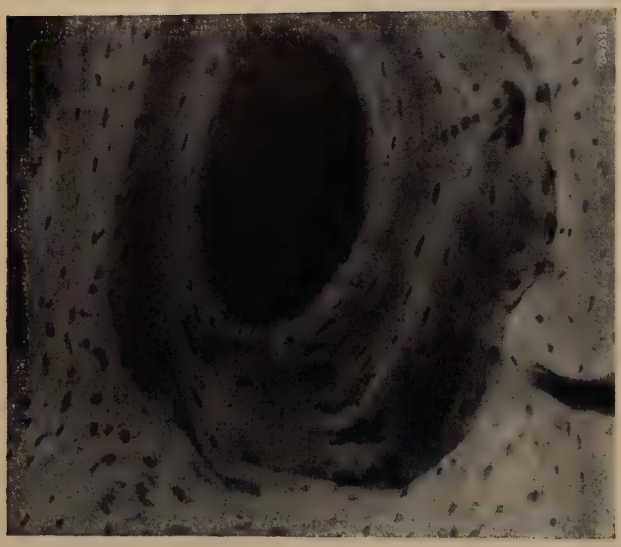

Fig. 12. Bone tissue around a blood vessel. To take such a microradiograph it is not necessary to de-calcify the bone, as it is in optical microscopy; hence it is possible to obtain information on the distribution of mineral salts in the bone. (5 kV, 3 mA, "Maximum Resolution" film; exposure 25 min.)

With micrographs of this kind it is possible to study, owing to the high absorption coefficient of the element, the deposition of calcium in bone tissue. It was in this way that Engström discovered the nature of the bone disease "osteogenesis imperfecta": microradiographic examination showed that there was incomplete calcification of the bone at various places and sometimes even rupture of the bone tissue.

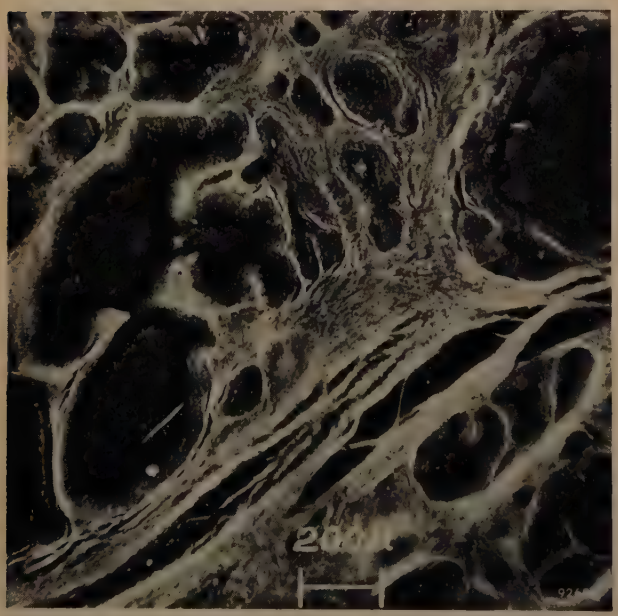

Fig. 13. Section (10 microns thick) of a hypertrophic prostate. The difference in the concentration of mineral salts in glandular and connective tissue is clearly visible. (3 kV, 3 mA, Eastman-Kodak "649-0" film; exposure 45 sec.) Explanatory note: the connective tissue appears very light, the glandular tissue grey; the large, very dark parts are due to the lumen, i.e. a space filled with fluid, generally serving for transport.

Examination of transparent objects

Just as it is possible to ascertain differences in chemical composition on optically opaque objects, it is also possible to do so on transparent objects. A good example is given in *fig. 13*. Without a complete chemical analysis the micrograph shows how the mineral salts have accumulated in the connective and not in the glandular tissue.

When there is very little or no contrast on the micrograph between various parts of an object in the natural state, contrast can sometimes be artificially produced with the aid of contrast media. For this purpose it is necessary to use substances containing heavy elements and which have the property of accumulating at very specific places instead of penetrating the object uniformly. For example, $AgNO_3$ is often used for showing up nerve fibres, Os compounds for fatty tissue and, for botanical specimens, I dissolved in KI solution, is used for staining starch.

An elegant application of this method is to follow what takes place during fixation with OsO_4. The latter — which is widely used in electron microscopy — is a slow process and brings about changes (naturally undesirable) in the specimen. In the long run, for instance, it causes the disappearance of the transverse bands of striated muscular tissue. A better insight into this process can be obtained by microradiographic examination [13]).

Determination of weight per unit area of biological objects

There are various methods of determining an object's weight per unit area. The most common is to radiograph, together with the specimen, a comparison object [14]), which may, for example, be a "step wedge" of collodion strips, laid upon the other, as shown in *fig. 14*. For this method it is necessary to have a not too small surface which is *homogeneously* irradiated by the X-rays. Not long ago a method was reported in which a comparison object is not required [15]). Several exposures of varying duration are made on a single film, and these give the relation between photographic density and exposure. Although a means of comparison is needed for obtaining the relation by which the mass can be derived from the transmission, all that is needed for this purpose is a layer of air of known thickness, temperature and pressure.

---

[13]) A. Recourt, Report of the Symposium on X-ray microscopy and microradiography, Cambridge 1956.
[14]) B. Lindström, Acta radiol., Suppl. **125**, 1955.
[15]) B. Combée and A. Engström, Biochim. biophys. Acta **14**, 432-434, 1954.

Quantitative chemical analysis

As already remarked, objects whose chemical composition is qualitatively known can be quantitatively analysed in their different details with the aid of microradiography. To determine the percentage content of a given element in the specimen, two micrographs are taken at wavelengths close to, but on different sides of, an absorption edge of that element. The percentage is derived from the ratio of the transmissions and the known variation of the absorption coefficient with the wavelength of the radiation [16]). For these measurements, then, a monochromatic X-ray beam is needed, which means that they cannot, without further measures, be carried out with the CMR 5 apparatus.

To sum up, it may be said that the CMR 5 apparatus constitutes a great advance towards the goal of making microradiography as simple a technique as optical microscopy. At a cost comparable to that of a good optical microscope, it has brought microradiography within the reach of many who have hitherto been deterred by the complicated equipment once required. The preparation of specimens takes less time than in optical microscopy, and represents no insuperable obstacle to the use of microradiography for routine pathological work. Moreover, it calls for no technique that was not already familiar in optical microscopy.

The salient features of the new apparatus are: 1) the use of a sealed-off X-ray tube, 2) small and simple H.T. generator, 3) compact construction, 4) very small focus, hence such small geometric unsharpness that the resolution is determined solely by the film (0.5 micron approx.). The apparatus can be used for all the purposes discussed in the foregoing, except for quantitative chemical analysis.

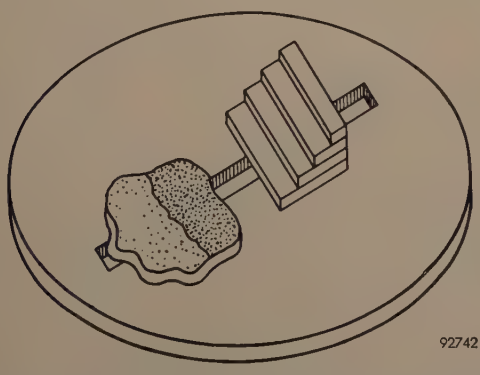

Fig. 14. Schematic representation of specimen carrier, showing specimen and collodium step-wedge side by side. From the known wieght per unit area of each step and the associated photographic density, a curve can be plotted with the aid of which the weight per unit area of a given part of the specimen can be found from the density of the corresponding part of the microradiograph.

[16]) See Part III of [14]).

Experiments with voltages lower than 1 kV

As we have seen, the resolving power of an emulsion is improved by the use of X-radiation of longer wavelength. It is interesting to see how this phenomenon continues at anode voltages still lower than the 1.5 kV limit with the CMR 5 apparatus. It has been found that at wavelengths corresponding to an anode voltage lower than 1000 V the smallest spacing that the types of films mentioned are capable of resolving is about 0.2 micron [17]). To derive full advantage from this high resolution, magnification by an optical microscope is no longer adequate and use must be made of an electron microscope.

For these experiments [18]) use was made of an X-ray tube of the type used in the CMR 5 apparatus, but without its window. Object and film were mounted in the normal way, except that the object was covered by an Al foil 0.1 to 0.2 micron thick to prevent light from the glowing cathode from reaching the film. The whole arrangement is shown schematically in *fig. 15*. In this way it is possible, without having to resort to extremely long exposures, to use anode voltages as low as 500 V. Naturally, this procedure meant that every time the film-holder was reloaded the tube had to be re-evacuated. *Fig. 16* shows two micrographs of a cavia oesophagus which were taken at anode voltages of 1000 and 850 V respectively (cf. fig. 2). *Figs 17* and *18* show the excellent resolution obtainable. Both represent a detail from fig. 16, the first magnified by an optical microscope, and the second by an electron microscope.

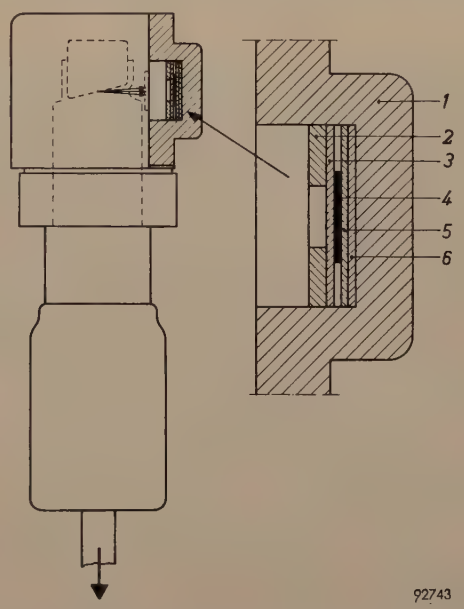

Fig. 15. X-ray tube and film-holder for contact microradiography at anode voltages lower than 1.5 kV. The tube is the same as that used in the CMR 5 apparatus, but the pump stem is not sealed off and the window is missing. In the film-holder (*1*) are mounted successively (seen from the target) the specimen mounting ring (*2*), a collodion film (*3*) carrying the specimen (*4*), on which an Al layer (*5*) is vapour-deposited to keep light from the cathode away from the film, and finally the film (*6*).

[17]) R. C. Greulich and A. Engström, Exptl. Cell Research **10**, 251-254, 1956.

[18]) See note [13]).

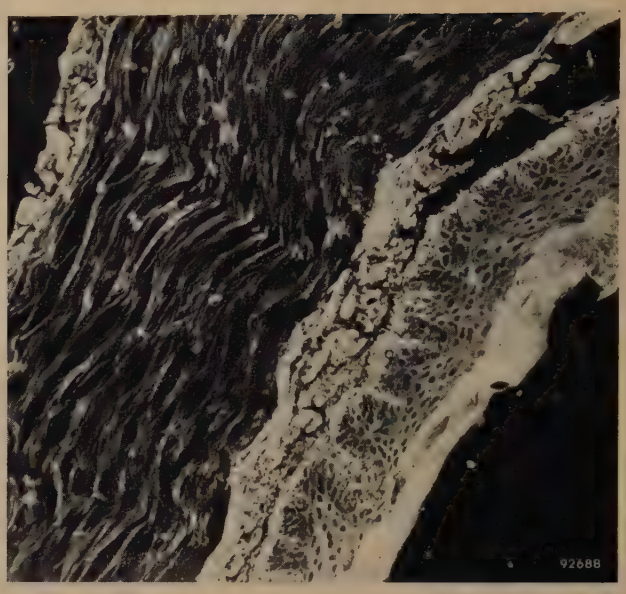

Fig. 16. Section of the oesophagus of a cavia, on the left taken at 1000 V, on the right at 850 V. It can be seen that the resolution is better than in the micrograph taken at 1.5 kV, shown in fig. 2. Magnification by optical microscope (130×).

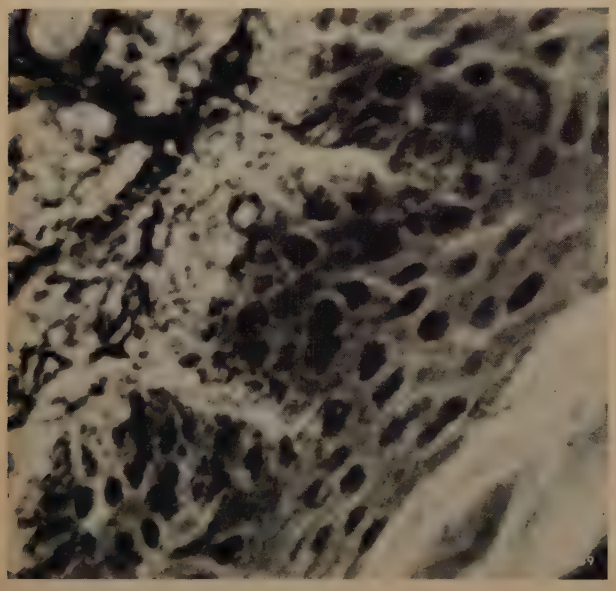

Fig. 17. Detail of 850 V micrograph in fig. 16. Magnification by optical microscope (600×).

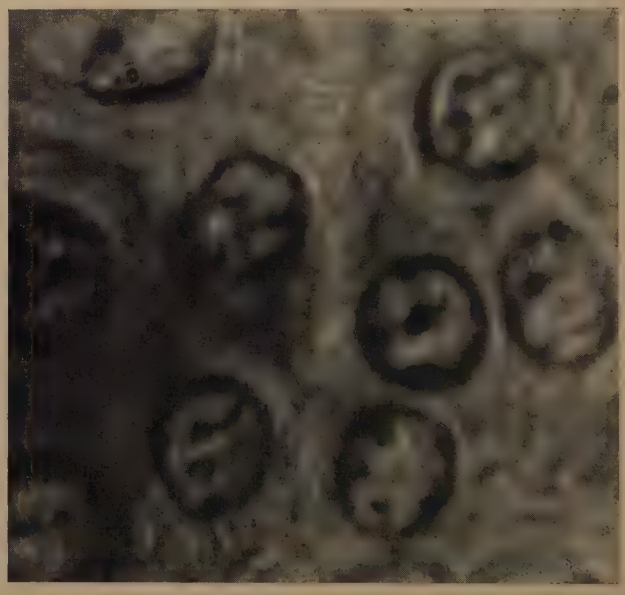

Fig. 18. Detail of 850 V micrograph in fig. 16. Magnification by electron microscope (2000×).

Magnification by an electron microscope introduces a new difficulty, since a film is too thick to act as an object for an electron microscope. As far as possible, all superfluous material must be removed (the celluloid film and the gelatine of the emulsion), leaving finally only the developed silver grains on a formvar film. This can be done, though the procedure — partly based on a technique of Comer and Skipper [19]) — is rather complicated.

[19]) J. J. Comer and S. J. Skipper, Science **119**, 441-442, 1954.

Summary. To make contrasty radiographs of thin sections of biological matter (e.g. 10 microns thick), it is necessary to use soft X-radiation. Such soft radiation cannot leave the X-ray tube unless the latter can be fitted with an exceptionally thin window of a material having a low atomic number. Until recently such windows could not be made vacuum-tight, and therefore the tube had to be continuously evacuated on a pump during the taking of an exposure. In latter years, however, it has proved possible to make a sealed-off X-ray tube, suitable for anode voltages from 1.5 to 5 kV, fitted with a beryllium window only 50 microns thick. A portable apparatus for contact microradiography (CMR 5), equipped with this tube, has now been developed. The apparatus contains a small H.T. generator for the anode voltage which can be varied continuously up to 5 kV. The tube current can also be regulated (max. 5 mA). The filament current is stabilized. When the H.T. is switched off, the filament voltage is automatically lowered to conserve the tube. Provisions are made for cooling the tube during long exposures and for evacuating the film-holder (e.g. with a water-jet pump) to prevent absorption of the X-rays in air. Since the focal spot is very small (0.3×0.3 mm) and film and object are in close contact, geometric unsharpness is negligible, and therefore the resolution is entirely determined by the resolution of the film. It is as good as 0.5 to 1 micron, which approaches that obtainable visually with an optical microscope (0.3 micron).

This means that an ordinary optical microscope is quite capable of providing the magnification required. Experiments are being carried out by several film manufacturers with a view to producing films with a better resolving power.

The procedure of preparing specimens is similar to that used in optical microscopy, but can be considerably simplified, reducing the time needed from 1-2 days to 1-2 hours. The particular value of microradiography is that it makes it possible to examine details in otherwise opaque objects (e.g. bone) and to gain an insight into more than merely the geometry of an object — for example the distribution of mineral salts in a tissue or the weight per unit area of particular details. If a monochromatic X-ray beam is available, the technique can also be employed for quantitative chemical analysis of separate details of an object. Examples of such problems are discussed with reference to the practice of histology and pathological anatomy.

Finally, some experiments are described in which no window is interposed between X-ray focus and object and the generating voltage is lower than 1 kV. With the soft X-radiation so produced, the films normally used for microradiography show a resolution as good as 0.2 micron. To take full advantage of this, the micrographs must be magnified with an electron microscope.

A MIRROR-CONDENSER LAMP FOR 8-mm PROJECTORS

621.326.732:778.55

To obtain a high luminous flux on the screen from 8-mm film projectors, designers tended until recently to use high-power lamps rather than to look for ways of improving the condenser optical system. The use of high-power lamps entails penalties in the size, weight and price of the projectors.

Closer examination of this problem in the Philips Laboratory at Eindhoven led to the conclusion that it must be possible to achieve the same result with a low-power lamp, by abandoning the conventional condenser optical system in favour of a small incandescent lamp having a partly silvered bulb, the latter being so designed as to serve as a mirror condenser. Experiments [1]) have confirmed this conclusion.

The lamp in question, which consumes only 50 watts (8 V, 6.25 A) is shown in *fig. 1*. *Fig. 2* represents a horizontal cross-section at filament level. The rear portion of the bulb has the form of an ellipsoid of revolution and is externally coated with a metal reflecting layer. The filament, a horizontal single spiral, is mounted at one focus of the ellipsoid, and a magnified image of the filament is formed at the other focus, which is situated about 12 mm beyond the front wall of the bulb. The film gate — 4.45 × 3.35 mm in 8-mm projectors — can now, without further optical components, be set up at about the position of the second focal point. It thus receives sufficiently uniform illumination from a beam of light having an aperture angle large enough for filling a projection lens of conventional speed (relative aperture f : 1.5) [2]). The front portion of the bulb is spherical in form and is silvered over an annular region as shown in fig. 1. By this means, some of the light emitted to the right (fig. 2), which would otherwise be lost, is reflected back on to the ellipsoidal mirror. Owing to the low power dissipation of the lamp, no forced cooling is required.

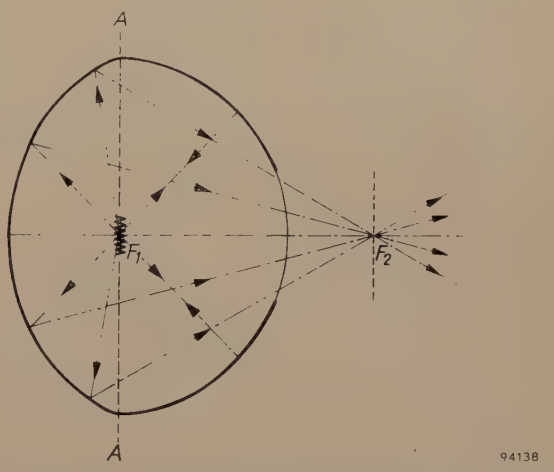

Fig. 2. Horizontal cross-section through mirror-condenser lamp at filament level. The section to the left of the line AA is part of an ellipse with foci F_1 and F_2. The section to the right of AA forms part of a sphere.

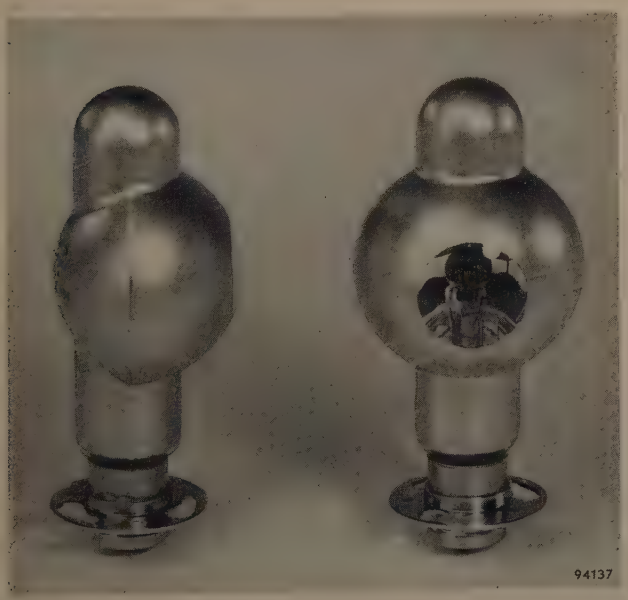

Fig. 1. Mirror-condenser lamp for 8-mm projectors. The total height of the lamp is 94 mm.

[1]) By F. L. van Weenen, who also posed the problem.

[2]) Elliptical mirror condensers have been used for other purposes (standard-film projection, airfield and stage lighting). See e.g. R. Sewig, Handbuch der Lichttechnik, part II, p. 710, Springer, Berlin 1938, and F. W. J. Schweigman, thesis, Groningen 1946.

Before discussing the details of this system, we shall briefly consider in general terms the two methods of arranging a condenser system to give intense uniform illumination of a projection aperture — and hence of a projection screen.

With the first arrangement (*fig. 3*), which is used as a rule for the projection of lantern slides, the condenser throws an image of the light-source on the projection lens and the diapositive is situated very close behind the condenser. This produces highly uniform illumination of the diapositive. If

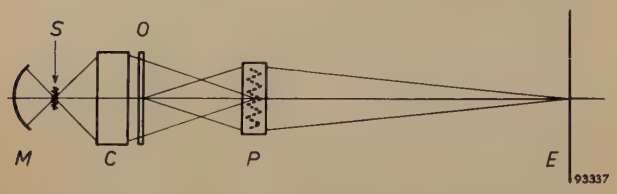

Fig. 3. Path of rays in a lantern-slide projector. The image of light-source *S* is formed in the projection lens *P*. The lantern slide *O* is immediately behind the condenser *C* and is thus uniformly illuminated. The auxiliary mirror *M* causes a somewhat larger fraction of the luminous flux emitted by the lamp to be usefully employed, but plays no part in the image formation. The projection lens projects the image of *O* on to the screen *E*.

this (physically ideal) system were to be used for the projection of very small pictures, and in particular 8-mm cine film, it would be necessary — assuming, that is, that loss of light at the film gate has to be kept to a minimum — to construct condenser lenses and light-sources of corresponding dimensions. Apart from the question of whether this would be technically feasible, it would still not be a satisfactory solution since condenser and film would be damaged by the heat generated by the light-source placed in such close proximity to them [3]).

The other arrangement, which is normally employed in film projectors, is illustrated in *fig. 4*. In this case the light-source is imaged in the film gate. Here, too, very little is lost of the light collected by the condenser, but the illumination of the film gate

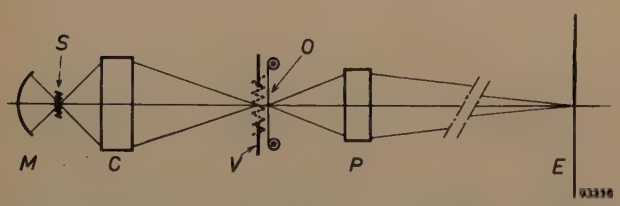

Fig. 4. Path of rays in a film projector. The image of the light-source *S* is formed near the film gate *V* by the condenser *C*. The auxiliary mirror *M* has the same function as in fig. 3. *P* projects the image of film *O* on to *E*.

[3]) In the projection of 35-mm film this drawback can be overcome by using a mercury-vapour lamp as light source. See Philips tech. Rev. **4**, 2-8, 1939.

is sufficiently uniform only if — assuming ideal image formation — the light-source has a surface of approximately constant brightness. Moreover, in order to limit light losses, this surface should be practically identical in form with the film gate.

With both these systems it is possible in principle to replace the condenser lenses by a mirror. It is even advantageous to do so, having regard to the solid angle subtended by the mirror at the filament. Mirrors with an aperture angle of 180° can readily be constructed, whereas not much more than 90° is possible with lenses, without incurring heavy costs. What is more, a mirror is, of course, free of chromatic aberration. In practice, however, the use of mirror condensers has so far been restricted to 35-mm projectors (with a carbon arc as light-source), the reason being that these condensers function satisfactorily only when their dimensions are large with respect to the light-source. If an incandescent lamp is used in conjunction with a separate mirror, the critical dimensions to be taken into account are rather those of the bulb than those of the filament: where the mirror employed is not large compared with the bulb a considerable fraction of the reflected light again passes once or twice through the bulb wall and undergoes, by refraction, changes in direction which distort the formation of the image. That, above all, is why it has hitherto not been practicable to use a mirror condenser in 8-mm projectors. Another drawback attaching to mirror condensers is that, in the long run, the reflecting surface becomes tarnished.

It is immediately evident from what has been said that these disadvantages do not apply to a lamp having the mirror directly coated on the bulb; tarnishing is no longer a problem and moreover the refraction of the light in the bulb is now of neglibible significance.

When the mirror-condenser lamp is used in conjunction with a projection lens having the relative aperture often used for 8-mm projection ($f:1.5$) the luminous flux incident on the screen is about 100 lumens. Suppose now we set up an incandescent lamp having the same filament luminance, together with an auxiliary mirror (see figs 3 and 4) and a normal condenser lens subtending an angle of, say, 90° at the filament. With the same projection lens as used above (this implies that the light from the condenser must converge at the same angle as before) and assuming the same overall reflection losses of 50% as estimated for the previous case, the luminous flux incident on the screen is the same as before (100 lumens). However, a larger filament will have been used: this follows from the

conditions that the light must just fill the film gate and converge at the same angle as before [4]). One may also say that, since a smaller fraction of the total light emitted is caught by the condenser lens and the filament has the same luminance as before, the same light flux through the system can be obtained only by using a larger luminous surface — which means a higher power. In the case cited (condenser subtending 90° at filament) the 100 lumens on the screen represents only $2\frac{1}{2}\%$ of the total light emitted by the filament (see *Table I*). In the case of the mirror condenser lamp, however, the 100 lumens represents about $4\frac{1}{2}\%$ of the total flux from the filament. It follows that the powers of the two lamps which, in the two cases, produce the same luminous flux on the screen are approximately inversely proportional to the above percentages.

In reality the power of the mirror-condenser lamp is even less than might be supposed from a comparison with other lamps on the basis of the above percentages, for the reason that the filament is brighter. This is achieved by the use of a low supply voltage: the filament is relatively thick so that, for a given useful life, a higher temperature is permissible than in high-voltage lamps. Because of the low power, a projector equipped with the new lamp requires only a relatively light transformer, and this, together with the absence of a cooling system, helps to keep down the weight of the projector.

Table I. The fraction of the emitted luminous flux reaching the projection screen when using a condenser lens subtending an angle of 90° (dimensions of filament adapted accordingly) compared with that when using the mirror-condenser lamp, both in conjunction with a projection lens having a relative aperture $f : 1.5$. The figures are only approximate, but they demonstrate the considerable gain obtained with the new lamp, owing to the large angle subtended by the condensing mirror at the filament.

	Condenser lens	Mirror-condenser lamp
Luminous flux emitted by lamp . . .	100%	100%
Fraction of the above collected by condenser (angle subtended by condenser lens 90°, by mirror-condenser lamp 160°) *)	30%	56%
Shutter transmits, say, one half the above	15%	28%
Due to overlap of the filament image and the non-ideal geometry [4]), the film gate transmits about $\frac{1}{3}$ of the above **)	5%	9%
Overall reflection losses at lens surfaces, lamp wall and condensing mirror here expressed as a percentage of the light flux that would otherwise emerge from the projection lens: approx. 50% ***). Hence total incident on screen	$2\frac{1}{2}\%$	$4\frac{1}{2}\%$

*) The percentages for both lens and mirror condensers are higher than would be expected from the effective solid angles they subtend: this is due to the use of the auxiliary spherical mirror.

**) Only when the dimensions of the filament are appropriate to the geometry of the condenser, may the same fraction ($\frac{1}{3}$) be taken in both cases.

***) Probably less in the set-up employing the new lamp.

The uniformity of illumination of the film gate is a result of several factors. In the first place, although the point where the filament intersects the axis of the ellipsoid is sharply focussed in the other focus of the ellipsoid, the off-axis parts are projected at slightly different positions by the different parts of the reflecting surface, i.e. they are imaged unsharply by the whole mirror (coma). In addition, depth of focus blurring occurs. In other words, although the cross-over of the light (where the beam has its smallest cross-section) lies at the second focal point, there is no question of a sharp image of the filament. It may also be deduced from the foregoing that uniformity of illumination of the film gate gives uniformity on the projection screen only provided that the projection lens contains the whole of the beam of light emanating from the film gate.

Since light-source and condenser form a single unit in the new lamp, a high degree of accuracy in dimensions must be achieved during fabrication. The lamp is provided with a type P15 pre-focussing base (see fig. 1). Each lamp is separately adjusted in an assembly jig, the filament being given a certain specified position with respect to the pre-focussing flange on the base; this having been done, the flange is soldered to the base [5]). Clearly, to obtain optimum results with the lamp, it is essential that the projector lampholder is also accurately positioned.

If we compare the properties that may be expected of an 8-mm projector equipped with the new lamp with those of the best existing projectors, we find that the number of lumens incident on the screen per kilogram weight of apparatus, and also the number of lumens per watt, are two to three times higher, an improvement, moreover, which is not obtained by using a very expensive lamp. On the contrary, the price of the lamp per lumen-hour is lower than that of other incandescent lamps for 8-mm projectors. The "price per lumen" of the whole projector will be even more favourable.

P. M. van ALPHEN,
M. BIERMAN.

[4]) See, for example, J. J. Kotte, A professional cine projector for 16-mm film, Philips tech. Rev. **16**, 158-171, 1954/55.

[5]) See Th. J. J. A. Manders, Philips tech. Rev. **8**, 72-81, 1946. This article also deals with other problems concerned with projection lamps.

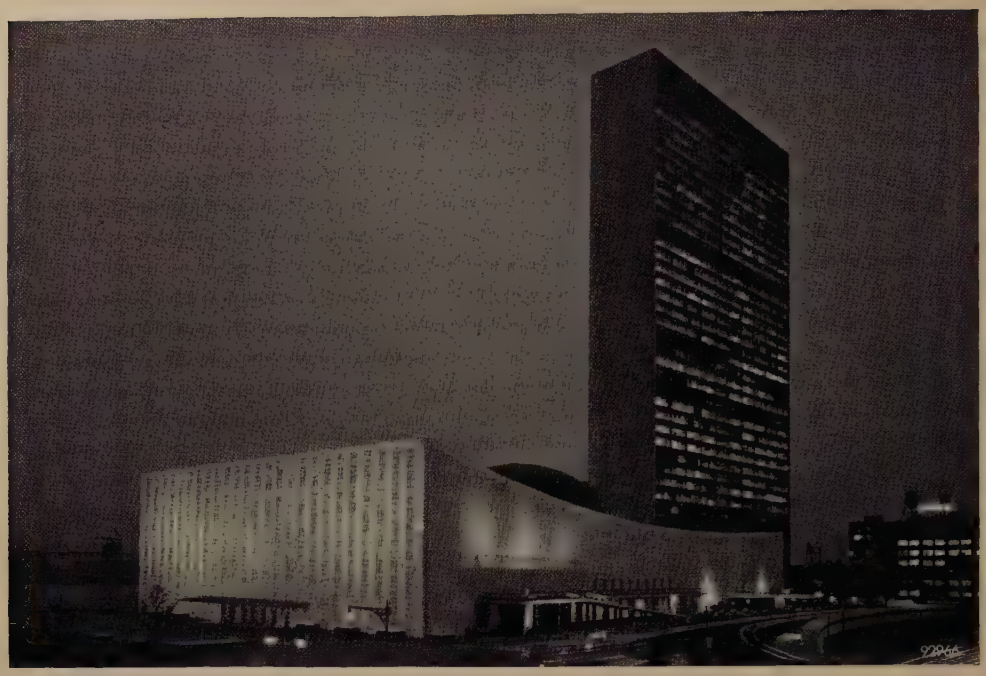

THE FOUCAULT PENDULUM IN THE UNITED NATIONS BUILDING IN NEW YORK

by J. A. HARINGX and H. van SUCHTELEN.

525.36.002.2

Among the gifts presented by member states for embellishing the United Nations building in New York is a large Foucault pendulum from the Netherlands. The pendulum, which is suspended in the entrance hall leading to the main Assembly Hall, continuously demonstrates by its movement that the earth is in rotation.

The article below briefly describes the suspension and driving systems of this pendulum. The design was based on the requirement that the pendulum should function well for a very long time without supervision and maintenance.

On 7 December 1955, Mr. H. Luns, Dutch Foreign Minister, presented to the Chairman of the United Nations General Assembly a Foucault pendulum on behalf of the people of the Netherlands. The pendulum is suspended above the central column of the staircase in the entrance hall of the United Nations building in New York (see *fig. 1*). The pendulum was specially designed in the Research Laboratory of N.V. Philips' Gloeilampenfabrieken, the guiding consideration being that the pendulum should function uninterruptedly for many years without requiring supervision or maintenance.

A Foucault pendulum is in principle merely a weight (which we shall henceforth refer to as the "bob") suspended by a long wire, swinging in a vertical plane. Owing to the manner of suspension the plane of swing is not, however, fixed with respect to the earth but, in consequence of the rotation of the earth, turns about the vertical through the point of suspension. In the northern hemisphere the plane of swing deviates in the clockwise direction, in the southern hemisphere in the opposite direction. It can be shown [1]) that for an idealized case (very long pendulum, very small amplitude) the time T' in which the plane of swing rotates 360° is given by the formula:

$$T' = \frac{T}{\sin \varphi}, \quad \ldots\ldots \quad (1)$$

in which T is the period of revolution of the earth and φ is the geographic latitude. At the poles $T' = T$, while at the equator $T' = \infty$, i.e. there is no rotation of the plane. In New York ($\varphi = 40°45'$), time $T' = 36$ hours 50 minutes. It further appears from the theory that the angular velocity with which the plane rotates with respect to the meridian is constant.

[1]) See e.g. A. Sommerfeld, Vorlesungen über theoretische Physik, Part I, Dieterich Verl., Wiesbaden 1952.

Fig. 1. The entrance hall in the United Nations building in New York. The Foucault pendulum, a gift from the Netherlands, is mounted above the central column of the staircase.

In practical conditions, the time of rotation is found from the formula:

$$T'' = \frac{T}{\sin \varphi}\left(1 - \frac{3}{8}\frac{a^2}{l^2}\right), \quad \ldots \quad (2)$$

in which a is the amplitude and l the length of the pendulum [2]). In the case of the pendulum in the United Nations building, l is about $17\frac{1}{2}$ m and a about 80 cm. This length gives a period of swing of approximately $8\frac{1}{2}$ sec. The weight of the pendulum bob is about 90 kg.

If we try to construct such a pendulum and repeat the celebrated experiment carried out by Foucault in 1851, a number of disturbing effects — due, for example, to imperfections in the rotational symmetry of the wire support — cause the pendulum, after some time, to execute an elliptical or even a circular motion. This had to be avoided with the present pendulum, which was required to swing continuously

[2]) Handbuch der Physik, Part V, p. 339, Springer, Berlin 1927.

without supervision. There were two other technical problems. In the first place there had to be the certainty that the wire would not break after some time of continuous operation, and in the second place a driving system was needed that would be able to provide the pendulum with sufficient energy to compensate for the loss of energy due to air resistance.

A simple method of overcoming the "ellipsing" problem has been described by Charron [3]). At a distance l' below the point of suspension A (see *fig. 2a*) he fixed a ring B having an internal diameter slightly larger than the thickness of the pendulum wire, leaving an annular spacing of d. As soon as the deflection of the bob exceeds the value ld/l', the wire touches the ring and the point of contact then functions as the "point of suspension". The consequence is that the minor axis of an elliptical orbit which may have been forming is rapidly diminished. With reference to fig. 2*b*, this can be roughly explained as follows.

Assuming that the wire, as long as it does not touch the ring, is straight, it will describe at the level of the ring an ellipse geometrically similar to the elliptical orbit of the bob reduced in the ratio l'/l. This is represented in the figure by the small broken ellipse; it is traversed, for example, in the direction of the arrow. The circle represents the limit set by the ring to the deflection of the wire. The moment the wire touches the ring, point B_1 functions as the point of suspension. Assuming that the velocity of the ball in the Y direction is small at that moment, the ball will thereupon proceed to describe the ellipse $CD'E'$, the axes of which lie along the lines B_1X' and B_1Y'. We see, then, that the amplitude

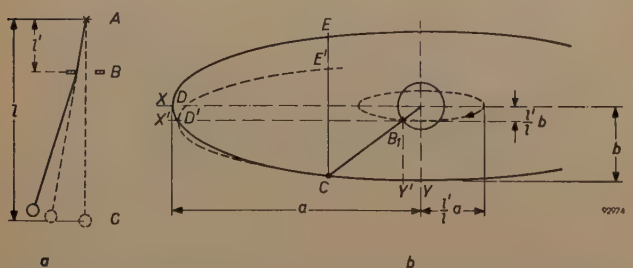

a b

Fig. 2. *a*) Suspension of pendulum according to Charron. The point of suspension is at A. The ring B, whose internal diameter is only slightly larger than the diameter of the wire, prevents the bob C from describing an ellipse.
b) Functioning of Charron's ring. When the pendulum describes an ellipse with semi-axes a and b, the wire touches the ring e.g. at point B_1. If there is sufficient friction between ring and wire, B_1 then functions for a while as the effective point of suspension and the bob describes the ellipse $CD'E'$ instead of the ellipse CDE, which it would describe in the absence of the ring. The amplitude in the Y direction is thus diminished in a half period by the length EE', which is equal to $2bl'/l$.

[3]) F. Charron, Bull. Soc. Astr. Fr. **45**, 457, 1931.

Fig. 3. The actual suspension system.

in the Y direction at the beginning of the following half swing has been reduced by the distance EE', which is approximately equal to $2bl'/l$. The relative reduction for each full swing amounts then to $\Delta b/b = 4l'/l$.

It has been tacitly assumed in the foregoing that while the bob describes the orbit $CD'E'$ the wire stays pressed against the ring at point B_1. As a rule the contact friction will not be sufficient for this to occur. In reality, therefore, $\Delta b/b$ is smaller than calculated here, but this does not alter the fact that the mounting of the ring is a very effective means of combating the elliptical motion.

Charron deduced that the use of this construction would slightly shorten the period of rotation and derived the following expression for the period:

$$T''' = \frac{T}{\sin\varphi}\left(1 - \frac{3}{8}\frac{a^2}{l^2} - \frac{4d}{\pi a}\right). \quad . \quad . \quad . \quad (3)$$

For the pendulum installed in New York a suspension was designed, wich, while equivalent to that of Charron, differs considerably in its construction. *Fig. 3* shows a photograph of the suspension and *fig. 4* a diagram indicating its construction. The mounting plate A, fixed on two beams, carries via three rods B a ring C. This ring supports by means of three flexible rods D a three-armed yoke E fitted with a universal joint F. The wire is suspended from F. By the bending of the flexible rods the yoke can move radially over a distance equal to the radial

play s between pin G and the periphery of a hole in the mounting plate. The flexible rods can be moved vertically and their length accurately adjusted; in this way the system as a whole can be given the required lateral stiffness and the pin made to lie exactly in the centre of the hole in the position of rest.

If we compare this arrangement with that of fig. 2*a*, we notice that the universal joint corresponds to the point of the wire which, in the Charron system, is at the height of the ring B. The hole in the mounting plate fulfils here the function of the ring, so that in the new construction the play s is equivalent to the play d in the old. The use of the universal joint avoids the friction and bending which the wire undergoes in Charron's construction at the level of the ring, thus greatly reducing the risk of wear or fatigue failure. The three flexible rods, like Charron's wire length AB, bear the weight G' of the pendulum bob etc. and, via the yoke, exert on the joint a centrally directed force which is proportional to the radial displacement. At a displacement u the above-mentioned point of Charron's wire is subjected to a force of magnitude Gu/l'. By appropriately dimensioning the flexible rods in the new construction, the same magnitude of restoring force can be produced.

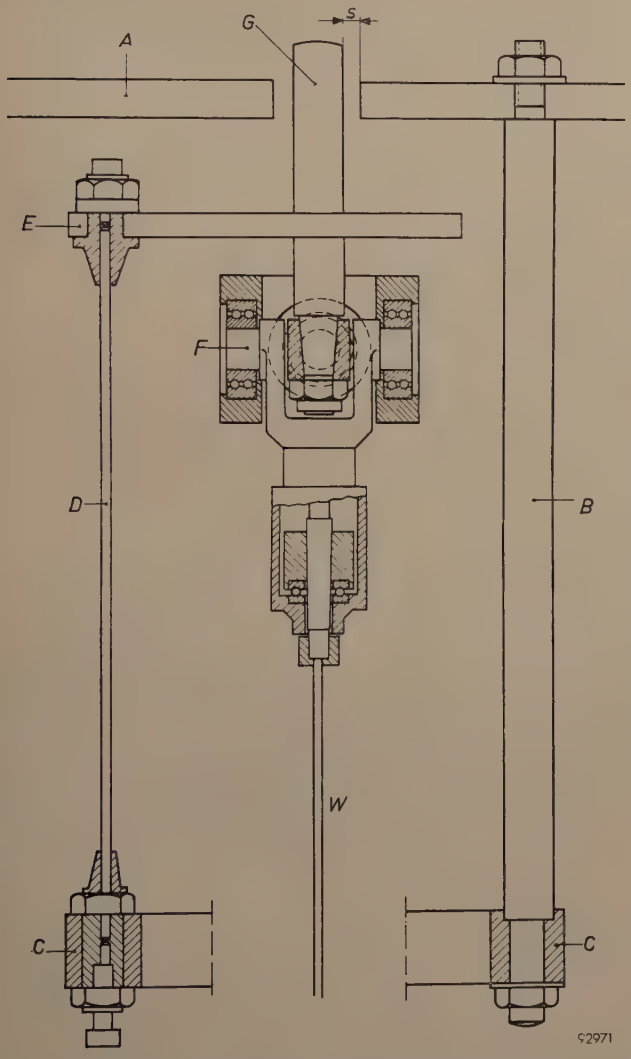

Fig. 4. Schematic diagram of the suspension system of the Foucault pendulum in the United Nations building. Mounting plate A carries three rigid rods B to which a ring C is fixed. Three flexible rods D, clamped on the latter, support a yoke E, which is fitted with a universal joint F. Pin G mounted on E, lies centrally in a hole in the mounting plate, and limits the lateral displacement of the yoke to the small distance s. The suspension wire W is fixed to the joint by clamping in a bifurcated steel cone. The dimensions of the flexible rods are such as to ensure the required lateral stiffness and to ensure that the bending stress in these rods is below their fatigue bending strength.

In connection with the dimensions of the flexible rods it should be borne in mind that the lateral stiffness c is determined not only by the dimensions and the modulus of elasticity but also to a large extent by the compressive force $\frac{1}{3}G'$. The length l' no longer corresponds to any physical quantity such as the length of the flexible rods, but is equal to $G'/3c$.

The lateral stiffness for this case (parallel-constrained ends) is given by the formula

$$c = \frac{P}{l_1} \frac{\frac{1}{2}ql_1}{\tan\frac{1}{2}ql_1 - \frac{1}{2}ql_1}, \quad \ldots\ldots \quad (4)$$

where $q^2 = P/EI$ and $P = \frac{1}{3}G'$. Further, l_1 is the length of the flexible rods, E their modulus of elasticity and I their second moment of area in bending.

The suspension wire is of hard drawn stainless steel with a diameter of 2.5 mm. The wire is clamped at both ends by a truncated cone of hardened steel with internal teeth. The cone has diametric saw cuts at its narrower end and is drawn fast into a ring by the weight of the bob.

In the design of the driving mechanism, which is necessary to keep the pendulum swinging without any reduction in amplitude, account had to be taken of the fact that access to the point of suspension is extremely difficult once the pendulum is mounted. The drive is therefore provided at the bob of the pendulum. The method adopted was to repel the bob by means of eddy currents generated in it by a coil mounted on the pedestal (*fig.* 5), the coil being energized at suitable moments by alternating current. If a copper plate is placed above such a coil at right angles to its axis, voltages will be induced in the plate which are 90° out of phase with the field, and currents which are in their turn almost 90° out of phase with these voltages. The eddy currents are therefore almost 180° out of phase with the current in the coil, thus giving rise to repulsion. If a not too large, horizontal, round plate is placed with its centre-point exactly in the axis of the vertical coil, the resulting force acting on the plate is a vertical one, but if the plate is slightly eccentric to the coil axis, the force will also have a horizontal component which can be used for driving the pendulum. A plate

Fig. 5. The pedestal, designed by architect G. Rietveld, on which the drive coil is mounted. The pedestal bears the inscription:

It is a privilege to live
This day and to-morrow.
Juliana

of this kind is contained in the lower half of the pendulum bob. In order to concentrate the magnetic field on the plate, 18 U-shaped yokes of ferroxcube are fitted around the coil.

This method, then, avoids the use of iron in the ball, and thus prevents the pendulum from being influenced by the magnetic field of the earth or by the steel structure of the building.

Some remarks may be added on the transfer of energy in this driving system. Eddy currents in the copper plate react on the coil with the result that the self-inductance of the latter is smaller than when the plate is absent. When the plate moves away this self-inductance increases and the energy transferred to the plate is approximately equal to $I^2\Delta L$, where ΔL is the change in the self-inductance and I the current. This does not take into account that I itself changes slightly, but, partly because of the circuit arrangement (see below), this relation holds fairly accurately.

The moment at which the coil is energized is determined by the moment at which the rod in the yoke (G, fig. 4) looses contact with the mounting plate [4]). For this purpose, rod and hole were designed to constitute an electrical contact. A delay circuit, which also controls the duration of energization, ensures that the current in the coil is switched on at a specific time after the moment the rod leaves the mounting plate, viz. at approximately the same moment at which the centre of the bob passes the axis of the coil. The anode load of tube II in the circuit (see *fig. 6*) includes the D.C. winding of a transductor T [5]). The A.C. winding L_1 of this transductor is connected in series with the drive coil L_2 and a capacitor C''. In addition, another capacitor C' is connected in parallel with L_1. When the D.C. coil of the transductor is not energized, the circuit L_1-C' is in resonance and represents such a high impedance that the current through L_2 is only 85 mA.

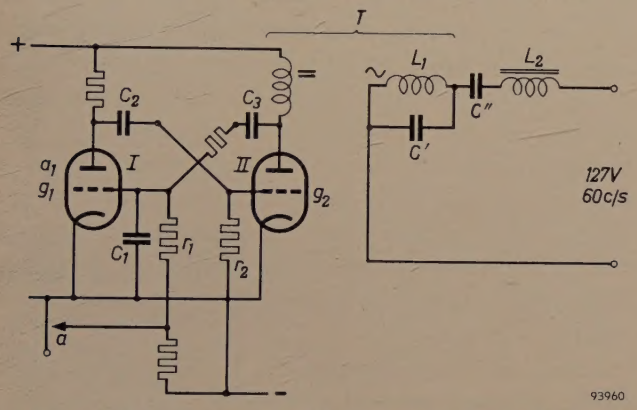

Fig. 6. Control and drive circuit for driving the pendulum. The control circuit (left) causes the required alternating drive current from the mains to be supplied to the drive coil L_2 only after a certain delay after the opening of contact a; the circuit sustains the current for a certain fixed time, even if contact a is again closed in the meantime. Contact a is formed by rod G (fig. 4) and the hole in the mounting plate A. In the quiescent state, tube I is conducting and tube II cut off. When a opens, the potential of g_1 falls and the potential of a_1 rises: at a certain point the circuit triggers, tube II now becoming conducting (via C_2) and tube I being cut off. The delay between the opening of a and the triggering of the circuit depends on the product C_1r_1. The anode current of tube II flows through the D.C. winding of transductor T and reduces the value of L_1 such that the drive circuit (right) comes into series resonance. After an interval, which depends on the products C_2r_2 and C_3r_1, the control circuit returns to the quiescent state and L_1 rises again. The value of C' is such that resonance now occurs in the parallel circuit L_1-C'. The latter then represents such a high impedance in the circuit that the current is reduced to an ineffective value.

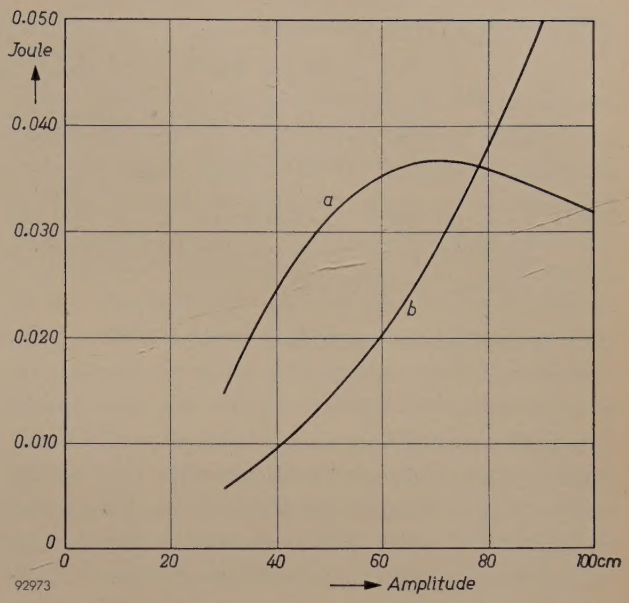

Fig. 7. The energy supplied per period to the pendulum (curve a) and that lost by air resistance (curve b) as a function of amplitude of swing. At an amplitude of approx. 80 cm the curves intersect. At smaller amplitudes the energy supplied is greater than that lost, i.e. the point of intersection represents a stable state of equilibrium.

When the transductor is energized by the anode current of tube II, the self-inductance of L_1 is reduced by about a half. The capacitance of C'' is such that the whole circuit now comes into series resonance, whereupon the current through L_2 rises to 240 mA. The ratio between operating and quiescent currents does not seem particularly large, but it must be remembered that the energy transferred is proportional to the square of the current. In this way about 0.035 joule is supplied to the bob in each period, which is sufficient to provide an amplitude of swing of the required value, viz. approximately 80 cm (see *fig.* 7).

Summary. A description is given of the suspension and driving systems for the Foucault pendulum suspended in the hall of the United Nations building in New York. The pendulum was presented on 7th December 1955 to the Chairman of the General Assembly by the Dutch Foreign Minister H. Luns on behalf of the people of the Netherlands. The main problem of preventing the pendulum bob from describing an ellipse instead of swinging in a flat plane was solved by utilizing the principle described by Charron. The construction is so designed as to reduce to a minimum the risk of the wire breaking owing to wear or fatigue. The drive, which is necessary to compensate for the energy losses, caused mainly by air resistance, is effected by means of a magnetic coil with ferroxcube core placed centrally under the pendulum. This coil is energized by alternating current and induces eddy currents in a copper plate contained inside the lower half of the bob. The energizing current is controlled by an electronic relay, which ensures that the current is switched on some time after the pendulum itself has broken an electrical contact in the suspension system, and keeps it switched on for a certain period. The coil is mounted on a pedestal designed by the architect G. Rietveld.

[4]) R. Stuart Mackay, Amer. J. Phys. **21**, 180, 1953, describes a pendulum driven by eddy currents, the synchronization being derived from the pendulum bob.

[5]) A transductor (saturable reactor) is a choke with an iron core, the self-inductance of which can be varied by changing the magnetization of the iron core with the aid of a D.C. winding.

ABSTRACTS OF RECENT SCIENTIFIC PUBLICATIONS BY THE STAFF OF N.V. PHILIPS' GLOEILAMPENFABRIEKEN

Reprints of these papers not marked with an asterisk * can be obtained free of charge upon application to Philips Electrical Ltd., Century House, Shaftesbury Avenue, London W.C. 2.

2482: C. A. de Bock, J. Brug and J. N. Walop: Antiviral activity of glyoxals (Nature **179**, 706-707, April 6, 1957).

In screening compounds for antiviral activity against influenza virus, a number of α-keto-aldehydes appeared to be active. The test compounds were injected in the allantoic cavity of 11 day embryonated hen's eggs, followed after 1 hr by the virus. After incubation for 48 hours the hæmagglutination (H.A.) titre of the allantoic fluid was estimated. A compound was considered active if the difference between the logarithm of this H.A. titre and that of a control was >0.6. Active compounds and the difference in log H.A. titre were CH_3COCOH (2.0), p-OH—C_6H_4COCOH (2.0), p-OH.m-NO_2—C_6H_3COCOH (2.3), p-Br—C_6H_4 $COCOH$ (0.7), m-NO_2—C_6H_4COCOH (2.1). The virus loses infective power when incubated with low concentrations (0.002 M) of glyoxals. At higher concentrations the glyoxals destroy the enzymatic activity of the virus. The virucidal action of the glyoxals is strong enough to explain the activity in the test.

2483*: H. de Lange Dzn.: Attenuation characteristics and phase-shift characteristics of the human fovea-cortex systems in relation to flicker-fusion phenomena (Thesis Delft, June 5, 1957).

The well-known frequency-response technique of systems analysis, in which the ratio of output amplitude to sinusoidal input amplitude is plotted against frequency in so-called attenuation characteristics, can successfully be applied to investigate the dynamic nature of the human visual organ from the retina up to the brain, using sinusoidally modulated light. This is possible because Talbot's law shows that, at flicker-fusion, the brightness-system works linearly. The internal threshold-value for flicker-fusion is supposed to be invariable with frequency at constant mean luminance and acts as a constant output value; the ripple-ratio $r =$ (amplitude of sinusoidal light variation)/(mean luminance) acts as a variable input of the brightness-system. This manner of investigation, previously applied in earlier papers with white light, is extended over nearly the whole range of cone-vision and is continued with coloured light. The existing theories on flicker-fusion provide no explanation for the shape of the attenuation characteristics obtained from the experiments and calculated from investigations by other authors. The attenuation charcteristics show at high luminance a pseudo-resonance effect, the bandwidth is greater and the slopes are such that for $r > 2\%$ the ratio (amplitude of fundamental)/(mean luminance) is decisive for flicker-fusion of any shape of interruption or modulation.

The well-known residual brightness-flicker just above the colour-flicker limit with heterochrome flicker-photometry with two anti-phase 100% sinusoidally modulated light beams can be reduced to zero by introducing an external phase correction $\Delta\psi$, which is found to be a function of luminance, colour difference and frequency. Subtracting logarithmically the attenuation characteristic of the colour-system from that of the brightness-system, it is found that the extra delay in colour-perception is identical to the filter-action of one integration process at high luminance; at low luminance a triple integration process occurs with the same time constant of 120 msec.

Using electrical analogues it is shown that the curves obtained are real attenuation characteristics of the brightness-system. In accordance with the pseudo-resonance peak in the attenuation characteristic for high luminance, an overshoot in the brightness perception occurs at about 1 c/s with perodic rectangular light impulses.

2484: A. Venema: The measurement of the pressure in the determination of pump speed (Vacuum 4, 272-283, 1954, No. 3, published Febr. 1957).

There is no commonly agreed method of determining the speed of a pump. One noteworthy method was proposed by Dayton in 1948 but it has not been accepted generally. Contributions to the problem made by other workers are briefly reviewed, followed by a close study of the basic elements of the definition of pressure. Special attention is given to the case where the number-density of the molecules varies along the mean free path. Such variation may occur at low pressures and exists, in particular, in the region of the pump mouth. The actual method of measuring pressure needs more consideration and it is shown that a gauge connected by a

tube to the system records the number of molecules per unit area arriving at the gauge-end of the tube. The conditions at the pump mouth have been investigated and an interpretation is given of the results of some measurements with regard to the distribution of the incident molecules. In conclusion, a method of measuring the speed of a pump is proposed which differs from Dayton's method. The new method is based on well-known concepts in the physics of gas flow at very low pressures. It has been put forward before, but simply as a postulate.

2485: M. H. de Lange: Heat transfer in glass furnaces from a theoretical and practical point of view (Travaux IVe Congrès int. du Verre, Paris, July 2-7, 1956, pp. 148-152; Chaix, Paris 1957).

An introductory survey is given of the various equations relevant to the calculation of the contribution of radiation to the transmission of heat through glass; certain equations relating to stationary conditions are also established. These equations are applied to the calculation of the vertical temperature distribution in a vat of glass. The equations are further applied to give an approximation to the effect of external cooling on the temperature of the inside wall of the furnace. An attempt is made to express the effect of radiated heat in non-stationary conditions, notably during the heating and the cooling of the glass.

2486: Y. Haven and J. M. Stevels: Note on the mechanism of ionic transport in glass (Travaux IVe Congrès int. du Verre, Paris, July 2-7, 1956, pp. 343-347; Chaix, Paris 1957).

Note drawing attention to information that can be derived from a comparison of diffusion and conductivity data, and to suggest that the mechanism of transport of Na^+ ions in glasses uses interstitialcies in certain cases (similar to the mechanism suggested by McCombie and Lidiard for Ag^+ in AgCl), whereas in other cases it is possible that vacancies are involved. The potential minima between the silicon-oxygen network available for the Na^+ ions are divided into sites — intersites and vacancies. Some examples are discussed which give some idea of the utility of the refinement of the theory given in this paper.

2487: A. Kats: The interaction of U.V. and X-rays radiation with silicate glasses and fused silica (Travaux IVe Congrès int. du Verre, Paris, July 2-7, 1956, pp. 400-411; Chaix, Paris 1957).

The formation of imperfections in silicate glasses and in fused silica under the action of X-rays has been studied. Optical absorption bands are observed in the region 2000-10 000 Å; they are attributable to centres which have captured electrons or holes. A number of alkali silicate glasses were irradiated at low temperature and measured at low temperature (80 °K). It is shown experimentally that the final result of the irradiation (either by u.v. of sufficient energy or by X-rays) is the loss of an electron by some of the oxygen ions or a displacement of the latter. It is still unknown via which intermediate transition states the centres are formed. Paramagnetic resonance measurements show the existence of electrons and holes attributable to the same centres as found optically. Imperfections in fused quartz after irradiation have also been investigated. It is shown that these may be due to centres originating from aluminium impurities.

2488: G. Diemer and W. Hoogenstraaten: Ambipolar and exciton diffusion in CdS crystals (Phys. Chem. Solids **2**, 119-130, 1957, No. 2).

The diffusion of photoconductivity in non-illuminated parts of CdS single crystals has been studied both on unactivated samples and on samples activated with Ag. Diffusion lengths ranging from a fraction of a micron to several hundreds of microns were observed. Measurements of the spectral response, the temperature dependence of the diffusion length and the P.E.M. (photo-electro-magnetic) voltage make it probable that the large values of the diffusion length are due to exciton diffusion. An activation energy of about 0.1 eV was found for thermal ionization of the excitons. At room temperature, in most of the Ag-activated crystals the thermal diffusion of the conductivity is a combination of ambipolar and exciton diffusion, a theory of which is given for a one-dimensional case.

2489: O. Reifenschweiler: Ionenquellen für kernphysikalische Untersuchungen (Elektrotechnik und Maschinenbau **74**, 96-103, 1957, No. 5). (Ion sources for nuclear research; in German.)

Survey of the more important ion sources used in nuclear research. The various types of sources are described, against the background of their common working princple. Some results of work on H.F. ion sources delivering currents of the order of 10 mA are given.

2490: N. W. H. Addink: Excitation energies in line spectra (Spectrochimica Acta **9**, 158-159, 1957, No. 2).

The calculation (according to Boltzmann's law) of the number of excited ions may not be carried out on the basis of simply adding the energies of ionization and excitation. The percentage of ions must first be determined (following Saha) and Boltzmann's distribution law then applied to the number of ions so found.

2491: S. Woldring: Continue onbloedige bloeddrukmeting bij de mens (Ned. T. Geneesk. **101**, 949-952, 1957, No. 20). (Continuous non-bloody blood-pressure measurement in man; in Dutch.)

Blood pressure in the arteries of the hand is measured on the principle of the "relaxed arterial wall". The pressure gradient established by the elastic tension of the arterial wall is overcome by compression of the surrounding tissues in a plethysmograph-like system, connected to a low-compliance manometer. Sample records of blood pressure under varying circumstances are given.

2492: J. H. N. van Vucht: Beitrage zur Kenntnis des Systems Cer-Aluminium (Z. Metallk. **48**, 253-258, 1957, No. 5). (Contribution to the study of the system cerium-aluminium; in German.)

The system Ce-Al was investigated by metallographic, thermoanalytical and X-ray diffraction methods for cerium concentrations above 50 at. %. Neither the compound Ce_2Al, nor the compound Ce_3Al_2, could be affirmed. Instead we discovered the existence of two modifications of a compound Ce_3Al. Below 230 °C, Ce_3Al has a hexagonal Ni_3Sn structure, above that temperature it is cubic with Cu_3Au structure. The compound CeAl was indexed as an orthorhombic one. A table with observed spacings and intensities is given.

2493: H. T. Schaap: De waterstofziekte van koper (Metalen **12**, 204-208, 1957, No. 11). (Hydrogen embrittlement of copper; in Dutch.)

A survey, with some results of the author's experiments, is given of the well-known effects of hydrogen embrittlement of copper. Copper containing more than 0.01 weight % oxygen becomes brittle when heated in hydrogen above 400 °C. Hydrogen diffusing into copper containing inclusions of Cu_2O reduces this oxide to metallic copper and water vapour. High pressures of water vapour are built up in this reduction causing local rupture along grain boundaries and resulting in embrittlement of the metal as a consequence of the fact that the rate of diffusion of hydrogen in copper is much higher than that of water vapour. In addition to these phenomena hydrogen embrittlement shows several other aspects, e.g. (*a*) cracks on the surface, (*b*) change of dimensions, (*c*) blisters on the surface, (*d*) series of holes along the grain boundaries, (*e*) holes in the interior of the grains. The conditions under which hydrogen embrittlement is encountered are described. Oxygen must be present as Cu_2O or as oxides from foreign metals whose affinity for oxygen is not much greater than that of copper and which show a measurable solubility in that metal. Our own experiments make it doubtful whether oxygen in solid solution may cause embrittlement. Small quantities of water vapour in the gas atmosphere can only be harmful in the presence of a material dissociating the water vapour, for instance chromium.

Now available

F. M. Penning: Electrical discharges in gases, Philips Technical Library, pp. viii+75, 29 figures.

This book is a translation of the Dutch original, which appeared in 1955, two years after the author's death. Although in recent years several new books have appeared on the subject of gas discharges, it is felt that the present book nevertheless fulfils a need, offering as it does a concise synopsis which can profitably be used by students as a basis for further study.

The contents are as follows: 1. Gas discharges, natural and man-made; 2. The conduction of electricity in metals and gases; 3. Non-self-sustaining discharges; 4. The movement of electrons and ions through a gas; 5. The non-self-sustaining arc discharge; 6. The Townsend discharge and breakdown; 7. Sparks and lightning; 8. The glow discharge; 9. The self-sustaining arc discharge; 10. The positive column. A bibliography and an index complete the book.